AD_____

Award Number: DAMD17-00-1-0081

TITLE: Targeting of Prostate Cancer with Hyaluronon-Binding Proteins

PRINCIPAL INVESTIGATOR: Lurong Zhang, M.D., Ph.D.

CONTRACTING ORGANIZATION: Georgetown University Medical Center
Washington, DC 20007

REPORT DATE: June 2002

TYPE OF REPORT: Annual

PREPARED FOR: U.S. Army Medical Research and Materiel Command
Fort Detrick, Maryland 21702-5012

REPORT DOCUMENTATION PAGE

Form Approved
OMB No. 074-0188

1. AGENCY USE ONLY (Leave blank)	2. REPORT DATE	3. REPORT TYPE AND DATES COVERED
	June 2002	Annual (1 Jun 01 - 31 May 02)

4. TITLE AND SUBTITLE
Targeting of Prostate Cancer with Hyaluronon-Binding Proteins

5. FUNDING NUMBERS
DAMD17-00-1-0081

6. AUTHOR(S)
Lurong Zhang, M.D., Ph.D.

7. PERFORMING ORGANIZATION NAME(S) AND ADDRESS(ES)
Georgetown University Medical Center
Washington, DC 20007

E-Mail: zhangl@georgetown .edu

8. PERFORMING ORGANIZATION REPORT NUMBER

9. SPONSORING / MONITORING AGENCY NAME(S) AND ADDRESS(ES)
U.S. Army Medical Research and Materiel Command
Fort Detrick, Maryland 21702-5012

10. SPONSORING / MONITORING AGENCY REPORT NUMBER

11. SUPPLEMENTARY NOTES
report contains color

12a. DISTRIBUTION / AVAILABILITY STATEMENT
Approved for Public Release; Distribution Unlimited

12b. DISTRIBUTION CODE

13. Abstract ***(Maximum 200 Words)*** *(abstract should contain no proprietary or confidential information)*

To test our **hypothesis** that the hyaluronan (HA) binding proteins (HABP) from cartilage is a new category of anti-tumor agents, we have proposed to focus on **three aims**: **1)** To examine the effect of HABP on the tumor growth of prostate cancer cell lines; **2)** To examine the effect of link protein and aggrecan on the tumor growth of prostate cancer; **3)** To examine the possible anti-angiogenesis effect of HABPs.

In past year, we have successfully finished the following works: **1)** cloned 993 bp of cDNA cording for N-terminus of human aggrecan, which consists of at least six HA binding motifs; **2)** inserted the cDNA into yeast expression vector; **3)** purified the recombinant human aggrecan for the media of transformed yeast; **4)** characterized that this recombinant aggrecan was highly glycosalated; **5)** demonstrated that the recombinant aggrecan could inhibit the proliferation of endothelial cells; and **6)** demonstrated that the recombinant aggrecan could inhibit the tumor growth *in vivo*.

We believe that this part of study is very meaningful: **1)** it determines that the aggrecan is an anti-tumor element in cartilage; **2)** the aggrecan in human form may be used directly in patients, if the effect is potent enough; **3)** the cDNA cloned in this study may be used for gene therapy.

14. SUBJECT TERMS	15. NUMBER OF PAGES
hyaluronan-binding proteins, experimental therapy, prostate cancer angiogenesis	22
	16. PRICE CODE

17. SECURITY CLASSIFICATION OF REPORT	18. SECURITY CLASSIFICATION OF THIS PAGE	19. SECURITY CLASSIFICATION OF ABSTRACT	20. LIMITATION OF ABSTRACT
Unclassified	Unclassified	Unclassified	Unlimited

Table of Contents

INTRODUCTION

Cartilage contains anti-tumor/angiogenesis substances, which has been widely used cancer patients as alternative medicine for more than two decades. However, it is unclear that which component in cartilage is responsible for its anti-tumor/angiogenesis effect. Since cartilage contains a large amount of hyaluronan (HA) and HA binding proteins (HABP), we **speculate** that HABP is responsible for the anti-tumor/angiogenesis effect of cartilage. This speculation is also based on the following observations: first, several proteins that bind to HA can also inhibit tumor growth or metastasis, such as soluble CD44 (1), RHAMM (2) and proteins from chondrocytes (3, 4); secondly, some angiogenic inhibitors, such as endostatin and angiostatin (5, 6), contain structural motifs that may allow them to bind to anionic proteoglycan (such as heparan sulphate and HA) and to interrupt the growth factor signaling (7).

To test our **hypothesis** that the hyaluronan (HA) binding proteins (HABP) from cartilage is a new category of anti-tumor agents, we have proposed to focus on **three aims**: **1)** To examine the effect of HABP on the tumor growth of prostate cancer cell lines; **2)** To examine the effect of link protein (LP) and aggrecan on the tumor growth of prostate cancer; **3)** To examine the possible anti-angiogenesis effect of HABPs.

The results of our **first year** study indicates that the HABP purified from cartilage with affinity column have the following properties: **1)** HABP can inhibit the anchorage-dependent and independent growth of tumor cells; **2)** HABP can inhibit proliferation and migration of endothelial cells *in vitro* and angiogenesis *in vivo*; **3)** HABP can reduce the growth of TSU prostate cancer and other tumor *in vivo*; **4)** HABP can inhibit the experimental lung metastasis; **5)** The anti-tumor effect of HABP is in part due to its anti-angiogenesis property. These results has been published in *Cancer Research* (2001; 61:1022-1028).

The HABP consists of two major subunits, the trypsin fragment of the core protein (aggrecan) and the link protein. Both of these subunits bind to each other as well as to HA. To dissect out which component is the responsible for the anti-tumor activity, we decide to use genetic engineering techniques to express the individual components in the human form. Since the bovine HABP is antigenic to human beings, it is not suitable for the long-term use in the patients with prostate cancer.

In this second year, the cDNA cording for human cartilage aggrecan were cloned, inserted into expression vector and then transfected into yeast. The recombinant human aggrecan was purified by Ni-column and tested for its HA binding activity, its effect on endothelial cells and its anti-tumor effect *in vivo*.

Our data suggest that aggrecan has an anti-tumor effect and it is the actual protein responsible for the anti-tumor effect of cartilage.

BODY

We have demonstrated that the cartilage HABP possesses anti-tumor/angiogenesis property. However, there are at least two major subunits in HABP that purified from HA affinity column: the trypsin fragment of the core protein (aggrecan) and the link protein. To dissect out which component is the responsible for the anti-tumor activity, we decide to use genetic engineering techniques to express the individual components in the human form. If these human proteins turn out to be anti-tumor/angiogenesis, then, they may have the potential to be utilized for cancer therapy, since the protein from human origin may have little antigenicity.

1. Construction, expression and purification of recombinant human aggrecan protein:

The aggrecan is one of the major HABPs in cartilage. The only way to obtain human aggrecan is to use molecular biology approach. According to the published cDNA sequence (GenBank access number M55172), we designed a pair of primers that framed from amino acid **V_{20} to T_{350}** in the N-terminal of aggrecan, which consisted of first 331 amino acids without signal peptide as elucidated in **Fig.1**.

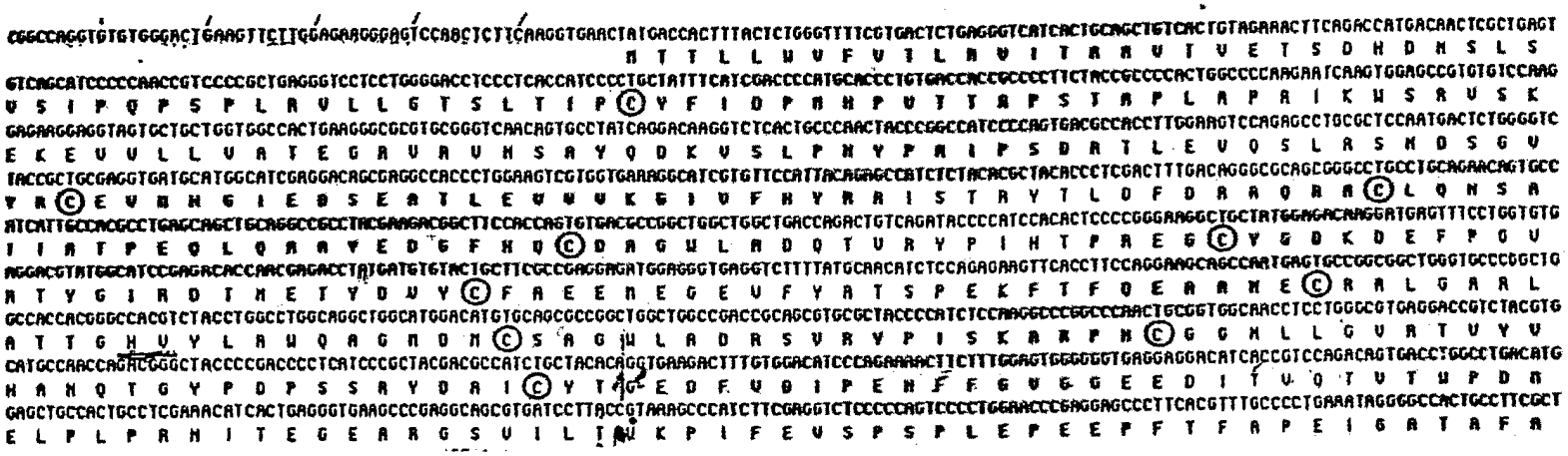

Fig.1. The N-terminal portion of human aggrecan. The first 19 amino acid is signal peptide and the wanted portion is from V_{20} to T_{350}.

The reason for cloning and expressing this portion (V_{20} to T_{350}) is that most of HA binding motifs of aggrecan is located in this region (**Fig 2**). It has been proved that there is a common shared and highly conserved motif, B[X7]B, in HABPs family. The B[X7]B is a minimal requirement for HA binding, and consists of two basic amino acids flanking a sequence of seven amino acids (8). The B (basic amino acids) can be either arginine (R) or lysine (K), which possess a positive charge under physical pH. The two basic amino acid and their spacing are critical for HA binding, which is convincingly confirmed by studies of site-directed mutagenesis and fusing protein from mutant cDNA (8).

This portion from V_{20} to T_{350} of human aggrecan that we wanted to clone had a theoretical pI/Mw: 5.33 / 36861.

VETSDHDNSLSVSIPQPSPLRVLLGTSLTIPCYFIDPMHPVTTAPSTAPLAP**RIKWSRVSKEK**EVVLL
VATEGRVRVNSAYQDKVSLPNYPAIPSDATLEVQSL**RSNDSGVYR**CEVMHGIEDSEATLEVVVKGI
VF**HYRAISTR**YTLDFDRAQRACLQNSAIIATPEQLQAAYEDGFHQCDAGWLADQTV**RYPIHTPR**E
GCYGDKDEFPGVRTYGIRDTNETYDVYCFAEEMEGEVFYATSPEKFTFQEAANEC**RRLGARLATT**
GHVYLAWQAGMDMCSAGWLAD**RSVRYPISKAR**PNCGGNLLGVRTVYVHANQTGYPDPSSRYDA
ICYT

Fig.2. HA binding motifs in N-terminus of aggrecan. It has six B[X7]B HA binding motifs.

After obtaining primers for the cloning the 331 amino acids of N-terminus of aggrecan, the RT-PCR was performed using a cDNA library of a human sarcoma cell line derived from chondrocytes as template. A correct RT-PCR product with a length of 993 bp was obtained (**Fig. 3**).

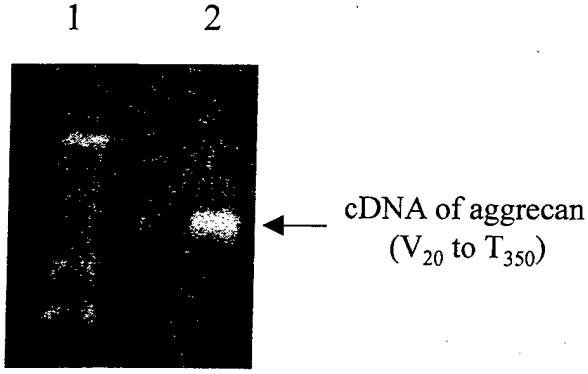

Fig. 3: The RT-PCR product for cDNA of aggrecan (V_{20} to T_{350}). Lane 1: Marker; Lane 2: A correct RT-PCR product with a length of 993 bp was obtained.

The cDNA cording for this portion of aggrecan (993 bp) was inserted into pPICZ yeast expression vector with α-factor signal peptide for secretion from yeast cells and His_6 tag for purification (**Fig. 4**).

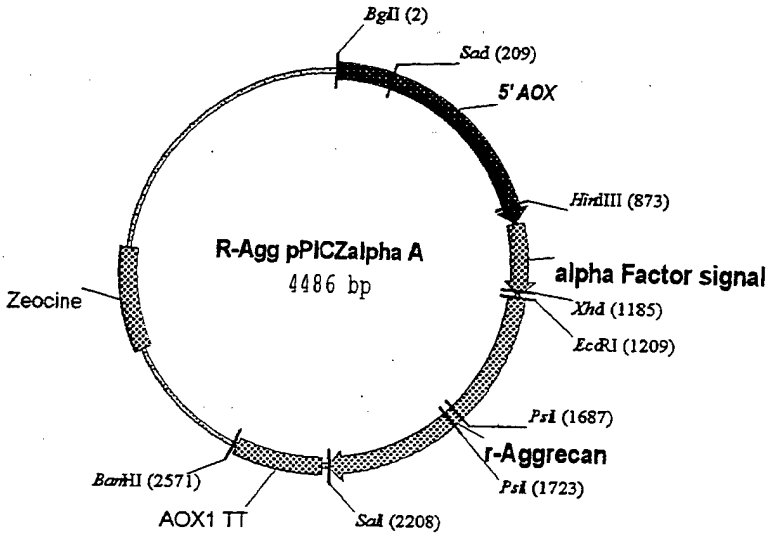

Fig. 4: The yeast expression vector for cloned human recombinant aggrecan. The α-factor signal peptide was used for secretion of human recombinant aggrecan from yeast into media. A His_6 tag in C-terminus was used for purification by Ni-column.

The correct cDNA and reading frame for human recombinant aggrecan was identified by sequencing. Then the yeast expression vector was transformed into two strains of yeast cells: X-33 and KM71, which allowed to obtain the different yields of recombinant aggrecan. Two clones from each strain were picked up for fermentation. The human aggrecan protein (**termed briefly as aggrecan**) secreted in the yeast culture media was purified with Ni-column. The purified aggrecan was subjected to electrophoresize on 8% SDS-PAGE gel, transfer to nitrocellulose membrane and stain with anti-His tag. To our surprise, the purified aggrecan had a very board ranges of apparent molecular weights (**Fig. 5**).

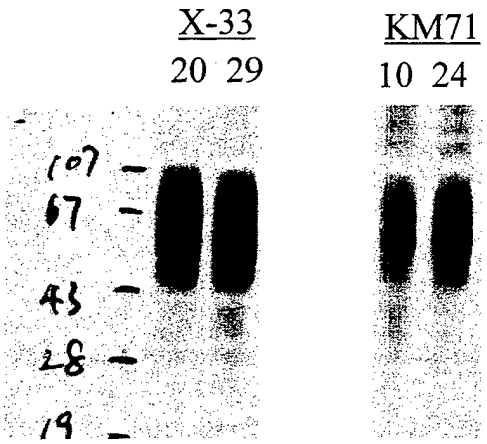

Fig. 5 The purified recombinant aggrecan. The purified recombinant aggrecan from four clones was subjected to electrophoresize on 8% SDS-PAGE gel, transfer to nitrocellulose membrane and stain with anti-His tag. The apparent molecular weight was in a very board ranges.

We speculated that this phenomenon may due to the expressed aggrecan was highly glycosylated. To confirm our speculation and make sure that the aggrecan protein was right, we decided to make a de-glycosylation form of aggrecan. For this, the three sites of asparagine (Asn, which is normally used for glycosylation) in aggrecan were changed into glycine by site-directed mutation (AAT or AAC to CAG). The vector that carried cDNA coding for de-glycosylation form of aggrecan was transformed into yeast. The purified de-glycosylation form of aggrecan was compared by with native aggrecan using Western blotting. The result (**Fig. 6**) did confirm that our speculation was right. The de-glycosylation form of aggrecan had a sharp band with a molecular weight about 37 kDa, which was different from its parental native glycosylation form.

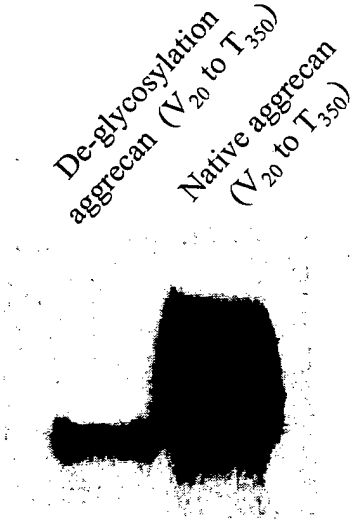

Fig. 6: Characterization of de-glycosylation form of aggrecan. Three sites of asparagine of aggrecan, which is normally used for glycosylation, were changed into glycine by site-directed mutation (AAT or AAC to CAG). The purified de-glycosylation form of aggrecan was compared by with native aggrecan using Western blotting. While the parental native glycosylated aggrecan had a very board ranges of molecular weight, the de-glycosylation form of aggrecan had a sharp band with a molecular weight about 37 kDa.

After confirming that we had the right protein of aggrecan, we decided to use native form, since the glycosylation may be needed for its bioactivity.

2. HA binding activity of human recombinant aggrecan.

The basic property of aggrecan is to bind to HA. To determine if the purified human recombinant aggrecan possesses this property, the HA binding assay was carried out. Twenty μl of biosynthesized ^{3}H-HA (5 X 10^5 cpm/μg HA, made by Dr. Charles B. Underhill in our Cancer Center) was mixed with 10 μg of human recombinant aggrecan or Metastatin (bovine HABP purified from nasal cartilage using HA affinity column, as positive control) without (as test) or with 50 fold excess of cold HA (as competition control), incubated for 1hr, applied to nitrocellulose membrane on dolt blot apparatus, and washed 5 times with PBS to get rid off free ^{3}H-HA. Each membrane circle with bound human recombinant aggrecan-^{3}H-HA was cut out individually and counted for radioactivity. The results (**Fig. 6**) showed that both recombinant aggrecan

and Metastatin had a strong ^{3}H-HA binding activity, which could be blocked by 50 fold excess of cold HA, suggesting that recombinant aggrecan do have its bioactivity.

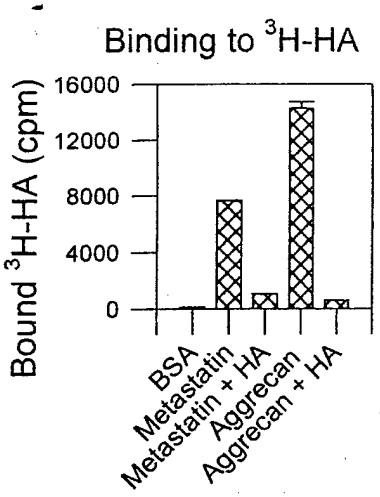

Fig. 6: Binding of human recombinant aggrecan to HA. Ten μg of purified recombinant aggrecan or Metastatin (as positive control) was mixed with 20 μl of biosynthesized ^{3}H-HA (5 X 10^5 cpm/μg HA) without (as test) or with 50 fold excess of cold HA (as competition control), incubated for 1hr, applied to nitrocellulose membrane on dolt blot apparatus and washed 5 times with PBS to get rid off free ^{3}H-HA. The bound ^{3}H-HA was counted with β-counter. The result indicated that recombinant aggrecan do have its bioactivity.

3. Effect of aggrecan on endothelial cells

Our previous study has showed that the Metastatin, purified HABP from bovine cartilage has strong anti-angiogenesis effect, which is responsible for its anti-tumor activity (9). To see if this is possessed by human recombinant aggrecan, 100 μg/ml of aggrecan or Metastatin (as positive control) was added to media of HUVEC (human umbilical vein endothelial cells) cultured in 96 well plate for two day and then added 30 μCi/well of ^{3}H-TdR. After 8 hours, the cells were harvested with 96 auto-harvester and the incorporated ^{3}H-TdR was counted with a β-counter. The result (**Fig. 7 A**) indicated that the recombinant aggrecan had a strong inhibitory effect on the proliferation of endothelial cells. To confirm that this effect was not due to the other contamination in the preparation of aggrecan, the aggrecan was heated to 100 °C to destroy the protein conformation and then tested with ^{3}H-TdR proliferation assay. The result (**Fig. 7 B**) showed that after the heat-inactivation, inhibitory effect of the aggrecan on proliferation of HUVEC was disappeared, suggesting that the natural structure of the aggrecan is required for its anti-endothelium activity. The difference between the test and the control was statistically significant ($p<0.05$).

A **B**

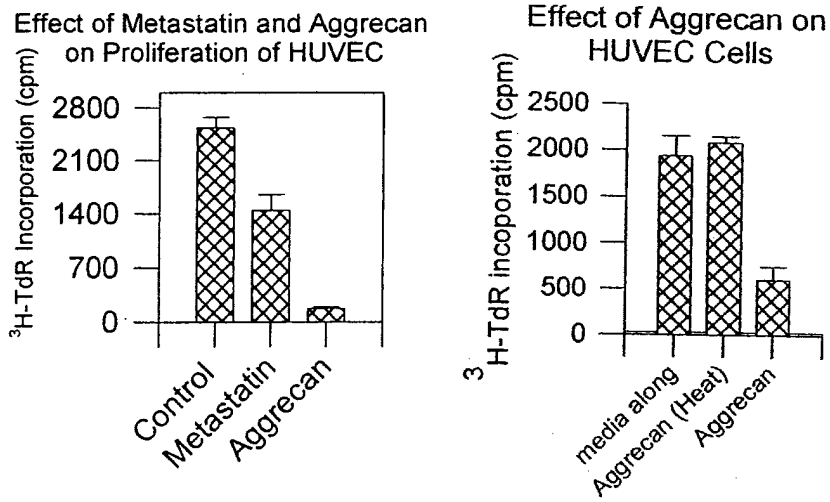

Fig. 7 Effect of recombinant aggrecan on endothelial cells. 100 μg/ml of aggrecan or Metastatin (as positive control) was added to media of HUVEC (human umbilical vein endothelial cells) cultured in 96 well plate for two day and then added 30 μCi/well of ^{3}H-TdR. After 8 hours, the cells were harvested with 96 auto-harvester and the incorporated ^{3}H-TdR was counted with a β-counter. **A:** Inhibitory effect of aggrecan on HUVEC; **B:** The action specificity of aggrecan: the natural structure of the aggrecan is required for its anti-endothelium activity.

4. In vivo anti-tumor effect of aggrecan

We were eager to see the effect of aggrecan on tumor growth. Two million of TSU tumor cells (recently this cell line was identified as bladder cancer cells, not a prostate cancer cell line, 10) were placed on top of CAM of 10 days old chicken embryos. Two days later, 100 μg of aggrecan was i.v. injected into CAM and four days later, the tumors were harvested, pictured and weighted. The results showed that the tumors in the aggrecan treated group were smaller than the control (**Fig. 8A**) and the difference in the tumor weight between two groups was statistically significant (**Fig. 8 B,** $P<0.05$). There was no difference in the chicken weight between two groups (**Fig. 8 C,** $P>0.05$), indicating that the aggrecan was not toxic to the embryo and did not impair the normal development.

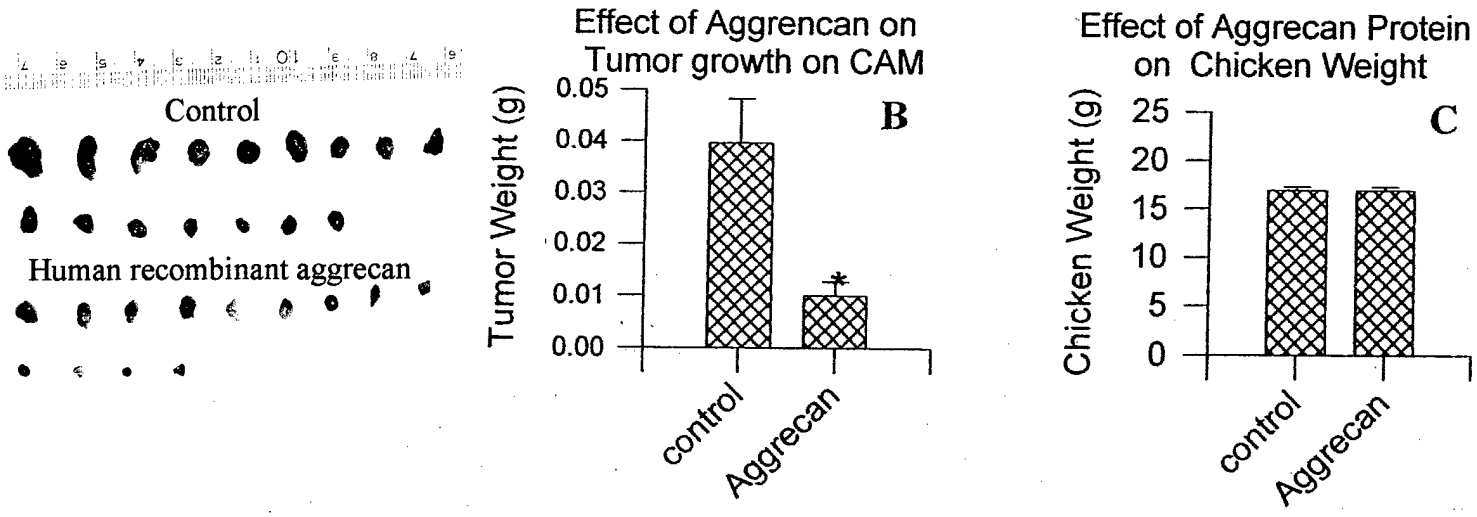

Fig 8. In vivo anti-tumor effect of aggrecan. Two million of TSU tumor cells were placed on top of CAM of 10 days old chicken embryos. Two days later, 100 μg of aggrecan was i.v. injected into CAM and four days later, the tumors were harvested, pictured and weighted. **A**: Pictures of TSU tumors; **B**: Tumor weights; **D**: Weights of chicken embryos. Compared to the control, the aggrecan strongly inhibited the tumor growth in vivo ($P<0.05$), but not impairing the normal development ($P>0.05$).

In summary, in past year, we have successfully finished the following works: **1)** cloned 993 bp of cDNA cording for N-terminus of human aggrecan, which consists of at least six HA binding motifs; **2)** inserted the cDNA into yeast expression vector; **3)** purified the recombinant human aggrecan for the media of transformed yeast; **4)** characterized that this recombinant aggrecan was highly glycosylated; **5)** demonstrated that the recombinant aggrecan could inhibit the proliferation of endothelial cells; and **6)** demonstrated that the recombinant aggrecan could inhibit the tumor growth *in vivo*.

We believe that this part of study is very meaningful: **1)** it determines that the aggrecan is an anti-tumor element in cartilage; **2)** the aggrecan in human form may be used directly in patients, if the effect is potent enough; **3)** the cDNA cloned in this study may be used for gene therapy.

Next year, we will further test: **1)** if the effect of recombinant aggrecan is dose-dependent; **2)** if link protein, an other component of HA binding protein from cartilage, also possess anti-tumor effect; **3)** the mechanism underlying the anti-tumor effect of HABPs from cartilage.

Key Research Accomplishments

Taken together, **in past year**, we have successfully finished the following works: **1)** cloned 993 bp of cDNA cording for N-terminus of human aggrecan, which consists of at least six HA binding motifs; **2)** inserted the cDNA into yeast expression vector; **3)** purified the recombinant human aggrecan for the media of transformed yeast; **4)** characterized that this recombinant aggrecan was highly glycosylated; **5)** demonstrated that the recombinant aggrecan could inhibit the proliferation of endothelial cells; and **6)** demonstrated that the recombinant aggrecan could inhibit the tumor growth *in vivo*.

We believe that this part of study is very meaningful: **1)** it determines that the aggrecan is an anti-tumor element in cartilage; **2)** the aggrecan in human form may be used directly in patients, if the effect is potent enough; **3)** the cDNA cloned in this study may be used for gene therapy.

Next year, we will focused on: **1)** if the effect of recombinant aggrecan is dose-dependent; **2)** if link protein, an other component of HA binding protein from cartilage, also possess anti-tumor effect; **3)** the mechanism underlying the anti-tumor effect of HABPs from cartilage.

Conclusions

- The N-terminus of aggrecan has HA binding activity and can be obtained as a recombinant protein from yeast with glycosylation.
- Aggrecan is an anti-tumor element in cartilage. It may responsible for the anti-tumor effect that we observed in the first year.
- The recombinant human aggrecan may be useful for clinical trial, if it has potent anti-tumor effect.
- The cDNA cloned in this study may be used for gene therapy.

Reportable outcomes

(Due to or partially due to this support)

Papers

1. Ningfei Liu, Feng Gao, Zeqiu Han, Charles B. Underhill and Lurong Zhang: Over-expression of Human Hyaluronan Synthetase 3 in TSU Prostate Cancer Cells Promotes Tumor Growth. Cancer Res. 2001; 61: 5207-5214

2. Hamada T, McLean WH, Ramsay M, Ashton GH, Nanda A, Jenkins T, Edelstein I, South AP, Bleck O, Wessagowit V, Mallipeddi R, Orchard GE, Wan H, Dopping-Hepenstal PJ, Mellerio JE, Whittock NV, Munro CS, van Steensel MA, Steijlen PM, Ni J, Zhang L, Hashimoto T, Eady RA, McGrath JA.: Lipoid proteinosis maps to 1q21 and is caused by mutations in the extracellular matrix protein 1 gene (ECM1). Hum Mol Genet 2002; 11(7): 833-840

3. Feng Gao, Zeqiu Han, Ivan Ding, Ningfei Liu, Weiming Liu, Jianzhong Xie, Charles B. Underhill and Lurong Zhang,: Hyaluronidase acts as a switch for fibroblast growth factor. (International J. Cancer cells, in press)

4. Liu N, Shao L, Xu X, Chen J, Song H, He Q, Lin Z, Zhang L, Underhill CB.: Hyaluronan metabolism in rat tail skin following blockage of the lymphatic circulation. Lymphology 2002; 35 (1):15-22

Abstracts

1. Xue-Ming Xu, Jinguo Chen, Luping Wang, Xu-Fang Pei, Shanmin Yang, Charles B. Underhill and Lurong Zhang: Peptides derived endostatin and angiostatin inhibits tumor growth. Proc. Annu. Meet. Am. Assoc. Cancer Res 2002; 43:1084:5364

2. Luping Wang, Jianjin Wang, Jiyao Yu, Haoyong Ning, Xu-Fang Pei, Jinguo Chen, Xue-Ming Xu, Shanmin Yang, Charles B. Underhill, Lei Liu and Lurong Zhang: Expression pattern of ECM1 in human tumors. Proc. Annu. Meet. Am. Assoc. Cancer Res 2002; 43: 729: 3618

3. Luping Wang, Xu-Fang Pei, Jinguo Chen, Xue-Ming Xu, Shanmin Yang, Ningfei Liu, Charles B. Underhill and Lurong Zhang: A peptide derived from hemopexin-like domain of MMP9 exerts anti-tumor effect. Proc. Annu. Meet. Am. Assoc. Cancer Res 2002; 43: 159:794

4. Shanmin Yang, Jinguo Chen, Xue-Ming Xu, Luping Wang, Shimin Zhang, Xu-Fang Pei, Jing Yang, Charles B. Underhill and Lurong Zhang: Triptolide, a potent anti-tumor/metastasis agent. Proc. Annu. Meet. Am. Assoc. Cancer Res 2002; 43: 854: 4233

5. Yixin Chen, Shuigen Hong, Ningfei Liu, Xu-Fang Pei, Luping Wang, Shanmin Yang[1], Xue-Ming Xu, Jinguo Chen, Charles B. Underhill and Lurong Zhang: Targeted hyaluronan binding peptide inhibits the growth of ST88-14 Schwann cells. Proc. Annu. Meet. Am. Assoc. Cancer Res 2002; 43: 888:4404

References

1. Sy, M-S., Guo, Y. J., and Stamenkovic, I.: Inhibition of tumor growth in vivo with a soluble CD44-immunoglobulin fusion protein. J. Exp. Med. 1992; 176: 623-627
2. Mohapatra S, Yang X, Wright JA, Turley EA, Greenberg AH: Soluble hyaluronan receptor RHAMM induces mitotic arrest by suppressing Cdc2 and cyclin B1 expression. J Exp Med 1996;183(4):1663-8
3. Moses, M A, Sudhalter, J., and Langer, R.: Identification of an inhibitor of neovascularization from cartilage. Science 1990; 248: 1408-1410
4. Moses, M A, Sudhalter, J., and Langer, R.: Isolation and characterization of an inhibitor of neovascularization from scapular chondrocytes. J. Cell Biol. 1992: 119 (2):473-482
5. O'Reilly MS. Boehm T. Shing Y. Fukai N. Vasios G. Lane WS. Flynn E. Birkhead JR. Olsen BR. Folkman J.: Endostatin: an endogenous inhibitor of angiogenesis and tumor growth. Cell 1997; 88(2):277-85
6. O'Reilly MS, Holmgren L, Shing Y, Chen C, Rosenthal RA, Moses M, Lane WS, Cao Y, Sage EH, Folkman J: Angiostatin: a novel angiogenesis inhibitor that mediates the suppression of metastases by a Lewis lung carcinoma. Cell 1994;79(2):315-28
7. Hohenester E. Sasaki T. Olsen BR. Timpl R.: Crystal structure of the angiogenesis inhibitor endostatin at 1.5 A resolution. EMBO Journal 1998; 17(6):1656-64
8. Yang B, Yang BL, Savani RC, Turley EA: Identification of a common hyaluronan binding motif in the hyaluronan binding proteins RHAMM, CD44 and link protein. EMBO J 1994;13(2):286-96
9. Ningfei Liu, Charles B. Underhill, Randall Lapevich, Zeqiu Han, Feng Gao, Lurong Zhang and Shawn Green: Metastatin: A hyaluronan binding complex from cartilage inhibits tumor growth. Cancer Res. 2001; 61:1022-1028
10. van Bokhoven A, Varella-Garcia M, Korch C, Miller GJ.: TSU-Pr1 and JCA-1 cells are derivatives of T24 bladder carcinoma cells and are not of prostatic origin. Cancer Res. 2001 Sep 1;61(17):6340-4.

[CANCER RESEARCH 61, 5207–5214, July 1, 2001]

Hyaluronan Synthase 3 Overexpression Promotes the Growth of TSU Prostate Cancer Cells[1]

Ningfei Liu, Feng Gao, Zeqiu Han, Xueming Xu, Charles B. Underhill, and Lurong Zhang[2]

Department of Oncology, Lombardi Cancer Center, Georgetown University Medical School, Washington DC 20007

ABSTRACT

Hyaluronan synthase 3 (HAS3) is responsible for the production of both secreted and cell-associated forms of hyaluronan and is the most active of the three isoforms of this enzyme in adults. In this study, the cDNA for human HAS3 was cloned and characterized. The open reading frame consisted of 1659 bp coding for 553 amino acids with a deduced molecular weight of about 63,000 and isoelectric pH of 8.70. The sequence of human HAS3 displayed a 53% identity to HAS1 and a 67% identity to HAS2. It also contained a signal peptide and six potential transmembrane domains, suggesting that it was associated with the plasma membrane. To evaluate the physiological role of human HAS3, expression vectors for this protein were transfected into TSU cells (a prostate cancer cell line), and the phenotypic changes in these cells were examined. The enhanced expression of hyaluronan in the transfected cells was demonstrated by dot blot analysis and ELISA. These cells were found to differ from their vector-transfected counterparts with respect to the following: (*a*) they grew at a faster rate in high (but not low) density cultures; (*b*) conditioned media from these cells stimulated the proliferation and migration of endothelial cells; (*c*) when placed on the chorioallantoic membrane of chicken embryos, these cells formed large, dispersed xenografts, whereas the control transfectants formed compact masses; and (*d*) when injected s.c. into nude mice, the xenografts formed by HAS3 transfectants were bigger than those formed by control transfectants. Histological examination of these xenografts revealed the presence of extracellular hyaluronan that could act as conduits for the diffusion of nutrients. In addition, they had a greater number of blood vessels. However, the HAS3-transfected TSU cells did not display increased metastatic properties as judged by their ability to form lung masses after i.v. injection. These results suggested that the HAS3-induced overexpression of hyaluronan enhanced tumor cell growth, extracellular matrix deposition, and angiogenesis but was not sufficient to induce metastatic behavior in TSU cells.

INTRODUCTION

A number of studies have suggested that the production of hyaluronan is associated with the metastatic behavior of tumor cells (1–11); *e.g.*, Toole *et al.* (1) have shown that invasive tumors formed by V2 carcinoma cells in rabbits have higher concentrations of hyaluronan than noninvasive tumors formed by these same cells in nude mice. Similarly, Kimata *et al.* (2) found that a strain of mouse mammary carcinoma cells with a high metastatic potential produced significantly greater amounts of hyaluronan than a similar strain with a low metastatic potential. In a previous study (3), we found that the amount of hyaluronan on the surfaces of mouse B16 melanoma cells was directly correlated with their ability to form lung metastases. Finally, increased levels of hyaluronan production have been correlated with a variety of metastatic tumors, including carcinomas of the breast, lung, liver, pancreas, and kidney (Wilms' tumor) (4–9). Indeed, in the case of Wilms' tumor (10) and mesotheliomas (11), the increased levels of hyaluronan in the serum of these patients has been regarded as a diagnostic marker for the clinical course of these conditions. Thus, there appears to be a correlation between hyaluronan production and metastatic behavior.

At present, three closely related isoforms for HAS[3] have been described, termed HAS1, 2, and 3, each of which appears to be associated with the plasma membrane (12–19). They have a predicted molecular mass of approximately 63 kDa, and transfection of cells with expression vectors for each of these isoforms can induce the synthesis of hyaluronan and the formation of a pericellular coat. However, the three isoforms are distinguished from each other with respect to: (*a*) their expression pattern during embryonic development and distribution in adult tissues; (*b*) the phenotype of knockout mutants in mice in which loss of HAS2 resulted in an embryonic lethality, whereas ones deficient in HAS1 and HAS3 were viable and had no obvious phenotype; (*c*) the rate at which they carry out hyaluronan synthesis, with HAS3 being more active than either HAS1 and HAS2; and (*d*) the size of the hyaluronan produced by the different isoforms with HAS3 giving rise to a somewhat smaller product than either HAS1 or 2 (17, 18).

Several recent studies have shown that transfection of tumor cells with expression vectors for hyaluronan synthase alters their behavior; *e.g.*, Kosaki *et al.* (20) reported that the transfection of human fibrosarcoma cells with HAS2 enhanced both anchorage-independent growth and tumorigenicity. In addition, Itano *et al.* (21) have found that clones of mouse mammary cancer cells that had low levels of hyaluronan synthesis demonstrated decreased metastatic properties, which could be restored if the cells were transfected with an expression vector for HAS1.

In this study, we have cloned and characterized the full-length cDNA for human HAS3 and examined its potential role in tumor progression. An expression vector carrying HAS3 was transfected into TSU prostate cancer cells, and alterations in the phenotype of the resulting cells were examined. We found that the HAS3-induced overexpression of hyaluronan enhanced the rate of tumor cell growth both *in vitro* and *in vivo*. Xenografts of the HAS3-transfected cells grew faster and larger, demonstrated a hyaluronan-rich stroma and increased vascularization. However, transfection with HAS3 did not shift the TSU cells to a more metastatic phenotype, suggesting that hyaluronan alone is not sufficient for metastasis in the case of TSU cells.

MATERIALS AND METHODS

Cell Lines. The TSU human prostate cancer cell line was obtained from the Tumor Cell Line Bank of the Lombardi Cancer Center (Georgetown University, Washington DC) and maintained in 10% calf serum, 90% DMEM. ABAE cells were kindly provided by Dr. Luyuan Li (Lombardi Cancer Center, Washington DC) and were cultured in 10% fetal bovine serum, 90% DMEM containing 2 ng/ml basic fibroblast growth factor.

Received 12/18/00; accepted 4/25/01.

The costs of publication of this article were defrayed in part by the payment of page charges. This article must therefore be hereby marked *advertisement* in accordance with 18 U.S.C. Section 1734 solely to indicate this fact.

[1] Supported in part by National Cancer Institute/NIH (R29 CA71545), United States Army Medical Research and Materiel Command (DAMD 17-99-1-9031; DAMD 17-98-1-8099; PC970502) and Susan G. Komen Breast Cancer Foundation (to L. Z. and C. B. U.). The animal protocols used in this study were approved by the Georgetown University Animal Care and Use Committee.

[2] To whom requests for reprints should be addressed, at Department of Oncology, Lombardi Cancer Center, Georgetown University Medical School, 3970 Reservoir Road, NW, Washington DC 20007. Phone: (202) 687-6397; Fax: (202) 687-7505; E-mail: Zhangl@gusun.georgetown.edu.

[3] The abbreviations used are: HAS, hyaluronan synthase; ABAE, adult bovine aorta endothelial cells; b-HABP, biotinylated hyaluronan-binding protein from cartilage; RT-PCR, reverse transcription-polymerase chain reaction.

Cloning and Characterization of cDNA for Human HAS3. Oligonucleotide primers for PCR of a partial sequence of cDNA for human HAS3 were designed according to the published sequence of Spicer and McDonald (Ref. 17; GenBank accession no. U86409) and consisted of the following: 5′-TCCTACTTTGGCTGTGTGCAG and 3′-AGATTTGTTGATGGTAGCA-AT. A human brain cDNA library (Clontech, Palo Alto, CA) was used as a template, and PCR was performed to generate a 570-bp fragment of human HAS3 cDNA. This fragment was then used to probe the human brain cDNA library. Positive clones were isolated, amplified, and sequenced. The Mac-Vector program was used to carry out homologue analysis of the cloned human HAS3 with other human and mouse HASs.

Construction and Transfection of Human HAS3 Expression Vector. The cDNA for HAS3 was subcloned into the pcDNA3 mammalian expression vector (Invitrogen, Carlsbad, CA), and correct clones were identified by restriction endonuclease map analysis. The HAS3-pcDNA3 or pcDNA3 (control vector) were transfected into TSU cells using the calcium precipitation method (22). The clones that survived in 1 mg/ml of Geneticin (G418) (>100 individual clones in each case) were pooled and expanded for further characterization.

Characterization of Transfected Cells. The presence of HAS3 message was determined by RT-PCR using the GeneAmp RNA PCR kit (Perkin-Elmer, Branchburg, NJ). The primers consisted of the following: 5′-TCATGGTGGT-GGATGGCAACCGC and 3′-CTAAGCCACCTGATGTACGTCCA, which gave rise to a 283-bp reaction product with HAS3 and a 324-bp product with HAS1. The amplified sequences were analyzed by agarose gel electrophoresis followed by staining with ethidium bromide.

Two methods were used to determine hyaluronan production by the transfected cells. The first consisted of dot blot analysis of secreted hyaluronan, in which conditioned media from vector-TSU and HAS3-TSU cells that had been cultured at similar densities for 3 days were applied to nitrocellulose membrane using a dot blot apparatus. After washing with PBS containing 0.1% Tween 20, the membrane was blocked with 5% nonfat milk and 1% polyvinylpyrrolidone in PBS for 30 min. The hyaluronan was detected by sequential incubations in 1 μg/ml of b-HABP (23) for 1 h, 0.25 μg/ml of peroxidase-labeled streptavidin for 1 h, and finally a chemiluminescent substrate for peroxidase.

The second method for quantitation of hyaluronan consisted of a modified enzyme-linked assay (23). For this assay, a high-bound ELISA plate (Falcon, Lincoln Park, NJ) was coated with 100 μg/ml of crude human umbilical cord hyaluronan (Sigma Chemical Co., St. Louis, MO) in PBS at room temperature overnight and blocked with 10% calf serum, 90% PBS. The samples of conditioned media and cell lysates were adjusted to equal protein concentrations, and 25-μl samples were mixed with 100 μl of 50 μg/ml of b-HABP at 37°C for 1 h and then transferred to the hyaluronan-coated ELISA plate. The unbound b-HABP remaining in the sample mixture could then bind to the hyaluronan-coated plate and was detected by incubation with 0.5 μg/ml of peroxidase-labeled streptavidin followed by a peroxidase substrate consisting of H_2O_2 and azinobis (3-ethyl-benzthiazoline sulfonic acid) in 0.1 M Na citrate (pH 5.0). The plate was read at A^{405}, and the concentration of hyaluronan in the samples was calculated from a standard curve.

The expression of CD44 by the vector-TSU and HAS3-TSU cells was examined by Western blotting. For this, both low- and high-density cultures were harvested with EDTA in PBS, and equivalent amounts of protein were dissolved in Laemmli sample buffer under nonreducing conditions and electrophoresed on a 10% SDS polyacrylamide gel. The resulting gel was electrophoretically transferred to a sheet of nitrocellulose and stained for CD44 using the BU52 monoclonal antibody (The Binding Site, Birmingham, United Kingdom) as described previously (24).

Anchorage-dependent Growth. Aliquots of medium (10% calf serum, 90% DMEM) containing 5000 transfected cells were added to 24-well dishes. At various times, the cells were harvested in 5 mM EDTA in PBS, and the cell number was determined with a Coulter counter. In some experiments, the cells were grown in the presence of 2 to 200 μg/ml of high molecular weight hyaluronan (Lifecore Biomedical, Chaska, MN) for 7 days.

Colony Formation. Vector-TSU or HAS3-TSU cells (20,000) were suspended in 1 ml of 0.36% agarose, 10% fetal bovine serum, 90% DMEM and then immediately placed on top of a layer of 0.6% solid agarose with 10% fetal bovine serum, 90% DMEM. Two weeks later, the number of colonies larger than 50 μm in diameter was quantified using an Omnicon Image Analysis system (Imaging Products International, Chantilly, VA).

Endothelial Cell Proliferation and Migration. For the proliferation assay, 2×10^3 ABAE cells were subcultured into 96-well plates and allowed to grow overnight. The next day, the media was replaced with 150 μl of 1% calf serum, 99% DMEM along with 50 μl of conditioned medium from either vector-TSU or HAS3-TSU cells. After 36 h, 0.3 μCi of [^{3}H]thymidine was added to each well, and 8 h later the cells were processed with an autoharvester. The incorporated [^{3}H]thymidine was determined with a β-counter.

For the migration assay, 25-μl aliquots of 10% FCS, 90% DMEM containing 5×10^3 ABAE cells were added to bottom wells of a 48-well Boyden chamber (Nucleopore, Pleasanton, CA) and then covered with a nucleopore membrane (5-μm pore size) coated with 0.1 mg/ml gelatin (25). The top well chamber was assembled and inverted for 2 h to allow the cells to adhere to the bottom side of membrane and then turned upright. Conditioned medium (50 μl) from either the vector-TSU or HAS3-TSU cells was added to top wells of the chamber and incubated for 2 h. The membrane was removed, the bottom side was carefully wiped to remove cells that had not migrated, and then the cells on the topside were stained with Hema 3 (Biochemical Science, Swedenboro, NJ). The membrane was placed on a slide, and the number of cells that had migrated to the topside were counted in 10 random high-powered fields.

Tumor Growth and Metastasis Assay. Two assay systems were used to determine tumor growth *in vivo*. In the first assay, 2×10^6 vector-TSU and

```
                                  G TGC GTT CGC GGC TGC TTT GAC CTG GTG GGC GCC GCC TCC
GGC ACT GCA CCG AGG CGG GGC GCC AGC GCC CAG GTT GCT GGG CTG GCC TTG GCG CCC CCT
TCC CCT ACC CAG AGC GCA GGC AGG CAG GGG GGT CCC GCC GCG CCC CTT CAG CAT ATG CCG160
                                                                  M  P   2
GTG CAG CTG ACG ACA GCC CTG CGT GTG GTG GGC ACC AGC CTG TTT GCC CTG GCA GTG CTG 220
V  Q  L  T  T  A  L  R  V  V  G  T  S  L  F  A  L  A  V  L   22
GGT GGC ATC CTG GCA GCC TAT GTG ACG GGC TAC CAG TTC ATC CAC ACG GAA AAG CAC TAC 280
G  G  I  L  A  A  Y  V  T  G  Y  Q  F  I  H  T  E  K  H  Y   42
CTG TCC TTC GGC CTG TAC GGC GCC ATC CTG GGC CTG CAC CTG CTC ATT CAG AGC CTT TTT 340
L  S  F  G  L  Y  G  A  I  L  G  L  H  L  L  I  Q  S  L  F   62
GCC TTC CTG GAG CAC CGG CGC ATG CAA CGT GCC GGC CAG GCC CTG AAG CTG CCC TCC CCG 400
A  F  L  E  H  R  R  M  Q  R  A  G  Q  A  L  K  L  P  S  P   82
CGG CGG GGC TCG GTG GCA CTG TGC ATT GCC GCA TAC CAG GAG GAC CCT GAC TAC TTG CGC 460
R  R  G  S  V  A  L  C  I  A  A  Y  Q  E  D  P  D  Y  L  R  102
AAG TGC CTG CGC TCG GCC CAG CGC ATC TCC TTC CCT GAC CTC AAG GTG GTC ATG GTG GTG 520
K  C  L  R  S  A  Q  R  I  S  F  P  D  L  K  V  V  M  V  V  122
GAT GGC AAC CGC CAG GAG GAC GCC TAC ATG CTG GAC ATC TTC CAC GAG GTG CTG GGC GGC 580
D  G  N  R  Q  E  D  A  Y  M  L  D  I  F  H  E  V  L  G  G  142
ACC GAG CAG GCC GGC TTC TTT GTG TGG CGC AGC AAC TTC CAT GAG GCA GGC GAG GGT GAG 640
T  E  Q  A  G  F  F  V  W  R  S  N  F  H  E  A  G  E  G  E  162
ACG GAG GCC AGC CTG CAG GAG GGC ATG GAC CGT GTG CGG GAT GTG GTG CGG GCC AGC ACC 700
T  E  A  S  L  Q  E  G  M  D  R  V  R  D  V  V  R  A  S  T  182
TTC TCG TGC ATC ATG CAG AAG TGG GGA GGC AAG CGC GAG GTC ATG TAC ACG GCC TTC AAG 760
F  S  C  I  M  Q  K  W  G  G  K  R  E  V  M  Y  T  A  F  K  202
GCC CTC GGC GAT TCG GTG GAC TAC ATC CAG GTG TGC GAC TCT GAC ACT GTG CTG GAT CCA 820
A  L  G  D  S  V  D  Y  I  Q  V  C  D  S  D  T  V  L  D  P  222
GCC TGC ACC ATC GAG ATG CTT CGA GTC CTG GAG GAG GAT CCC CAA GTA GGG GGA GTC GGG 880
A  C  T  I  E  M  L  R  V  L  E  E  D  P  Q  V  G  G  V  G  242
GGA GAT GTC CAG ATC CTC AAC AAG TAC GAC TCA TGG ATT TCC TTC CTG AGC AGC GTG CGG 940
G  D  V  Q  I  L  N  K  Y  D  S  W  I  S  F  L  S  S  V  R  262
TAC TGG ATG GCC TTC AAC GTG GAG CGG GCC TGC CAG TCC TAC TTT GGC TGT GTG CAG TGT1000
Y  W  M  A  F  N  V  E  R  A  C  Q  S  Y  F  G  C  V  Q  C  282
ATT AGT GGG CCC TTG GGC ATG TAC CGC AAC AGC CTC CTC CAG CAG TTC CTG GAG GAC TGG1060
I  S  G  P  L  G  M  Y  R  N  S  L  L  Q  Q  F  L  E  D  W  302
TAC CAT CAG AAG TTC CTA GGC AGC AAG TGC AGC TTC GGG GAT GAC CGG CAC CTC ACC AAC1120
Y  H  Q  K  F  L  G  S  K  C  S  F  G  D  D  R  H  L  T  N  322
CGA GTC CTG AGC CTT GGC TAC CGA ACT AAG TAT ACC GCG CGC TCC AAG TGC CTC ACA GAG1180
R  V  L  S  L  G  Y  R  T  K  Y  T  A  R  S  K  C  L  T  E  342
ACC CCC ACT AAG TAC CTC CGG TGG CTC AAC CAG CAA ACC CGC TGG AGC AAG TCT TAC TTC1240
T  P  T  K  Y  L  R  W  L  N  Q  Q  T  R  W  S  K  S  Y  F  362
CGG GAG TGG CTC TAC AAC TCT CTG TGG TTC CAT AAG CAC CAC CTC TGG ATG ACC TAC GAG1300
R  E  W  L  Y  N  S  L  W  F  H  K  H  H  L  W  M  T  Y  E  382
TCA GTG GTC ACG GGT TTC TTC CCC TTC TTC CTC ATT GCC ACG GTT ATA CAG CTT TTC TAC1360
S  V  V  T  G  F  F  P  F  F  L  I  A  T  V  I  Q  L  F  Y  402
CGG GGC CGC ATC TGG AAC ATT CTC CTC TTC CTG CTG ACG GTG CAG CTG GTG GGC ATT ATC1420
R  G  R  I  W  N  I  L  L  F  L  L  T  V  Q  L  V  G  I  I  422
AAG GCC ACC TAC GCC TGC TTC CTT CGG GGC AAT GCA GAG ATG ATC TTC ATG TCC CTC TAC1480
K  A  T  Y  A  C  F  L  R  G  N  A  E  M  I  F  M  S  L  Y  442
TCC CTC CTC TAT ATG TCC AGC CTT CTG CCG GCC AAG ATC TTT GCC ATT GCT ACC ATC AAC1540
S  L  L  Y  M  S  S  L  L  P  A  K  I  F  A  I  A  T  I  N  462
AAA TCT GGC TGG GGC ACC TCT GGC CGA AAA ACC ATT GTG GTG AAC TTC ATT GGC CTC ATT1600
K  S  G  W  G  T  S  G  R  K  T  I  V  V  N  F  I  G  L  I  482
CCT GTG TCC ATC TGG GTG GCA GTT CTC CTG GGA GGG CTG GCC TAC ACA GCT TAT TGC CAG1660
P  V  S  I  W  V  A  V  L  L  G  G  L  A  Y  T  A  Y  C  Q  502
GAC CTG TTC AGT GAG ACA GAG CTA GCC TTC CTT GTC TCT GGG GCT ATA CTG TAT GGC TGC1720
D  L  F  S  E  T  E  L  A  F  L  V  S  G  A  I  L  Y  G  C  522
TAC TGG GTG GCC CTC CTC ATG CTA TAT CTG GCC ATC ATC GCC CGG CGA TGT GGG AAG AAG1780
Y  W  V  A  L  L  M  L  Y  L  A  I  I  A  R  R  C  G  K  K  542
CCG GAG CAG TCA AGC TTG GCT TTT GCT GAG GTG TGA CAT GGC CCC CAA GCA GAG CGG GTA1840
P  E  Q  S  S  L  A  F  A  E  V  *                                        553
AAG TGC AAT GGG TAA GGG AGG GAA GGG GAA TGG AAG AGA AAA GAC AGG GTG GGA GGG AGG1900
AGG GAG TGC TGT GTT TTA GTC TCT TAA TGG TCC AAA GGA CAA ATC TAA AAT GCA AAG AAC1960
GGT GAT GTA GTA TGG CCT GAC AGC TCT GTT TA                                  1992
```

Fig. 1. Nucleotide sequence and derived amino acid sequence of human HAS3. The open reading frame of human HAS3 consists of 1659 bp coding for 553 amino acids. The signal peptide (first 27 amino acids) and the six transmembrane domains are *underlined*. Between the first transmembrane domain (amino acids 43 to 65) and the second transmembrane domain (amino acids 384 to 402) there is a stretch of 319 amino acids located outside of the plasma membrane, which is probably the major functional region for the synthase activity. The remaining 170 amino acids in the COOH terminus (amino acids 384 to 553) contain five transmembrane domains that can form loops that span the plasma membrane. The GenBank accession no. is AF234839.

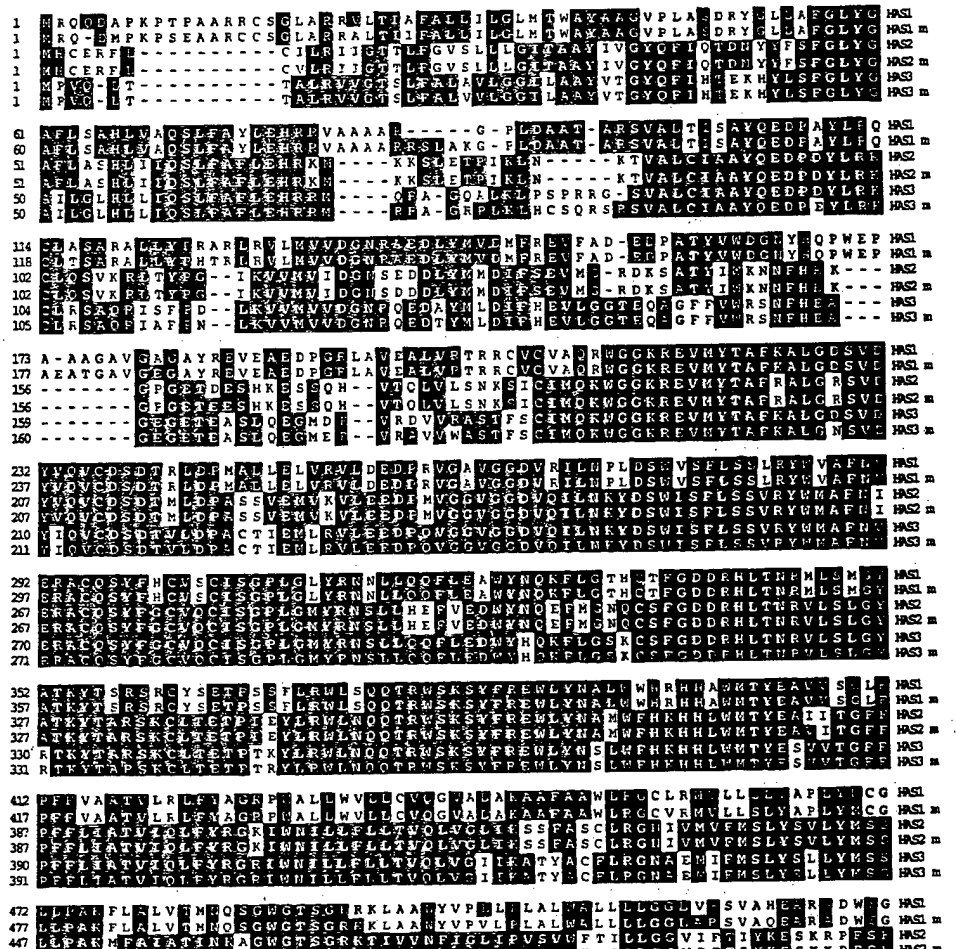

Fig. 2. Comparison of the human HAS3 with other members of the HAS family. Human HAS3 is about 53% identical to HAS1, 67% identical to HAS2 of both human and mouse (*m*), and 96% identical to mouse HAS3.

HAS3-TSU cells were placed on the chorioallantoic membranes of 10-day-old chicken embryos (15 eggs/group) and incubated at 37°C for 5 days. The tumor masses that grew on the chorioallantoic membranes were removed, photographed, and weighed. In the second assay system, the transfected cells were injected s.c. into 5-week-old male nude mice (2×10^6 cells/site; five mice/group), and the size of the xenografts was measured twice a week. At the end of 3 weeks, the mice were sacrificed, and the xenografts were photographed, weighted, and then fixed with 3.7% formaldehyde or frozen in liquid nitrogen for immunohistochemical staining.

To examine experimental metastasis, 5×10^5 vector-TSU and HAS3-TSU cells were injected into the tail veins of 5-week-old nude mice (five mice/group). Three weeks later, the mice were sacrificed, and the lungs were examined under a dissecting microscope for metastases.

Histological Staining. To stain cultured cells for hyaluronan, the transfected cells were seeded into an 8-well chamber slide (Nunc, Naperville, IL) and allowed to grow to confluence. After fixation in 3.7% formaldehyde for 5 min, the cells were washed and stained with 10 μg/ml b-HABP in 10% calf serum, 90% PBS, followed by 4 μg/ml of peroxidase-conjugated streptavidin and finally a substrate consisting of 3-amino-9-ethyl-carbazole and H_2O_2 that gives a dark red reaction product (23).

To stain xenografts for hyaluronan, the tissue was fixed with formaldehyde, embedded in paraffin, and cut into 5-μm thick sections. After the removal of the paraffin, the sections were processed as described above. After the immunoperoxidase reaction step, the sections were counter-stained with Mayer's hematoxylin and then preserved with Crystal/Mount (Biomeda, Foster City, CA).

To stain for endothelial cells, samples of the xenografts were rapidly frozen, cut into 10-μm thick sections, fixed in acetone, and air-dried. The sections were incubated sequentially with: (*a*) a 1:30 dilution of rat antimouse CD31 (PharMigen, San Diego, CA) in 10% calf serum, 90% PBS for 1 h; (*b*) avidin-biotin complex method reagents for rat IgG (ABC kits; Biomeda); (*c*) a peroxidase substrate consisting of H_2O_2 and 3-amino-9-ethyl-carbazole; and (*d*) counter-stained with Mayer's hematoxylin. The numbers of immunopositive spots corresponding to small blood vessels were counted in 10 random fields of three samples from each group.

Statistical Analysis. The mean and SE were calculated from the raw data and then subjected to Student's *t* test. The $P < 0.05$ was regarded as statistically significant.

RESULTS

Cloning and Characterization of Human HAS3. The full-length cDNA for HAS3 was cloned from a cDNA library of human brain using a probe consisting of a known partial sequence of the gene. The open reading frame contained 1659 bp coding for 553 amino acids and is shown in Fig. 1. The HAS3 protein had a deduced molecular weight of about 63,000 and a pI of 8.70. The first 27 amino acids represented

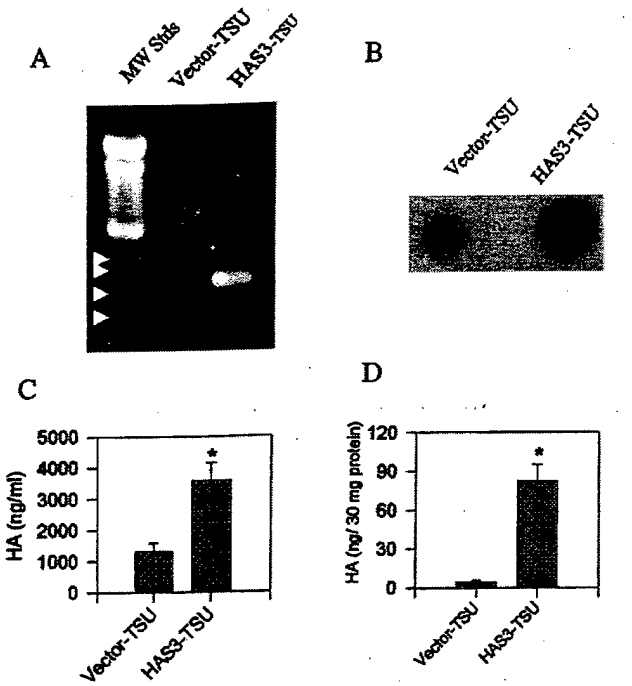

Fig. 3. Analysis of vector-TSU and HAS3-TSU cells for HAS3 mRNA and hyaluronan production. *A*, for the analysis of HAS3 message, RNA was extracted from the cultured cells and subjected to RT-PCR as described in "Materials and Methods." Agarose gel electrophoresis of the reaction products showed that the HAS3-TSU cells contained a prominent band of approximately 280 bp that was absent from the vector-TSU cells. The positions of markers for 100 through 400 bp are indicated by the *arrowheads* in the first *lane*. *B*, for the analysis of hyaluronan production, conditioned media from the transfected cells was applied to nitrocellulose using a dot blot apparatus and stained for hyaluronan using b-HABP, followed by peroxidase-labeled streptavidin and a chemiluminescence reagent. The dots represent the hyaluronan in conditioned media of vector-TSU cells (*left*) and HAS3-TSU cells (*right*). *C* and *D*, the amount of hyaluronan in conditioned media and cell lysates as determined by an ELISA are shown respectively. The increase of hyaluronan in conditioned media and lysates from HAS3-TSU cells as compared with the vector-TSU cells was statistically significant ($P < 0.05$).

the signal peptide (the cleavage site is between ILA and AY). There were six transmembrane sequences, one in the NH_2 terminus and five in the COOH terminus. Between the first transmembrane sequence (from amino acid 43 to 65) and second transmembrane sequence (from amino acid 384 to 402), there was a stretch of 319 amino acids located outside of plasma membrane, which appeared to be the major functional region for polysaccharide synthesis. The 170 amino acids in the COOH terminus (from amino acid 384 to 553) contained five transmembrane domains that can form loops spanning in and out of the plasma membrane. A potential *N*-glycosylation site was present at amino acid position 462, a glycosaminoglycan attachment site at position 464, and several phosphorylation sites for tyrosine kinase, casein kinase, protein kinase C, and cyclic AMP- and cyclic GMP-dependent protein kinases. HAS3 also contained seven hyaluronan-binding motifs of $B(X_7)B$ in which B is either R or K, and X_7 contains no acidic residues and at least one basic amino acid (26). Similar domains are present in other hyaluronan-binding proteins such as RHAMM, CD44, hyaluronidase, link protein, aggrecan, human GHAP, and TSG-6. Fig. 2 shows that compared with related enzymes, human HAS3 was about 53% identical to HAS1 (both human and mouse forms), 67% identical to HAS2, and 96% identical to mouse HAS3. These results are consistent with earlier studies of this and related genes (13–19).

Overexpression of Hyaluronan in TSU Cells Transfected with HAS3. To examine the role of HAS3 in tumor progression, the cloned cDNA was inserted into a mammalian expression vector (pcDNA3) under the control of a cytomegalovirus promoter and then transfected into TSU cells (human prostate cancer). To avoid complications associated with clonal variations, all of the clones (>100) that survived in 1 mg/ml of Geneticin (G418) were pooled and expanded for experimental analysis throughout this study. The presence of HAS3 message in the transfected cells was examined by RT-PCR as described in "Materials and Methods." When analyzed by agarose gel electrophoresis (Fig. 3*A*), the HAS3-TSU cells gave rise to a PCR product of approximately 280 bp corresponding to HAS3, whereas no such band was detected in the vector-TSU cells. In addition, no reaction product of 314 bp was apparent, indicating that the message for HAS1 was absent from these cells.

The production of hyaluronan by the transfected cells was initially examined by dot blot analysis. As showed in Fig. 3*B*, conditioned medium from HAS3-TSU cells contained a significantly greater amount of hyaluronan than that from vector-TSU cells. To quantitatively measure the hyaluronan, a competitive enzyme-linked assay was performed. Fig. 3, *C* and *D* show that both conditioned medium and lysates of HAS3-TSU cells contained greater amounts of hyaluronan as compared with those of the control vector-TSU cells. However, there was no obvious difference in the level of CD44, a cell surface receptor for hyaluronan, on the two cell types at either low or high density as determined by Western blotting (data not shown). Taken together, these results indicate that the transfection of TSU cells with cDNA for HAS3 stimulated their production of hyaluronan.

HAS3 Promotes Cell Growth at High Densities. We then compared the growth rates of the vector-TSU and HAS3-TSU cells. For this, the transfected cells were subcultured at similar starting densities, and at various times thereafter the cells were harvested and enumerated with a Coulter counter. Fig. 4*A* shows that during the first 4 days, there was no obvious difference in the proliferation rates of the vector-TSU and HAS3-TSU cells. However, after day 5, the HAS3-TSU cells began to proliferate at a faster rate than the vector-TSU cells. Thus, at high densities, the HAS3-transfected cells grew at a faster rate. This conclusion was also suggested by our recent finding that transfection of MDA-231 human breast cancer cells with antisense to HAS3 results in decreased expression of hyaluronan and inhibition of their growth at high densities.[4] Together, these results indicate that HAS3 plays a role in cell proliferation at high densities.

Cultures of the vector-TSU and HAS3-TSU cells were then compared with respect to their patterns of growth and hyaluronan staining. As shown in Fig. 4*B* (*top*), the vector-TSU cells displayed a cobblestone appearance indicative of contact inhibition of growth with relatively little staining of pericellular hyaluronan. In contrast, the HAS3-TSU cells (Fig. 4*B*, *bottom*) appeared to have lost contact-inhibition of growth, forming numerous multilayered clusters of cells, which were associated with most of the hyaluronan staining. In addition, the HAS3-TSU cells displayed an enhanced ability to form colonies in soft agar as compared with the vector-TSU cells (Fig. 4*C*). Thus, at high densities, the HAS3-transfected cells grew at a faster rate, presumably because they had partially lost contact inhibition of growth.

Conditioned Medium from HAS3-TSU Stimulated the Proliferation and Migration of Endothelial Cells. Because several studies (27–29) reported that hyaluronan can modulate angiogenesis, we examined the effects of conditioned medium from HAS3-TSU cells on the behavior of cultured endothelial cells. When conditioned medium from HAS3-TSU cells was added to the medium of ABAE cells, it stimulated their proliferation by 66% as compared with that from vector-TSU cells (Fig. 5*A*). Furthermore, conditioned medium from the HAS3-TSU also stimulated the migration of ABAE cells through

[4] Unpublished data.

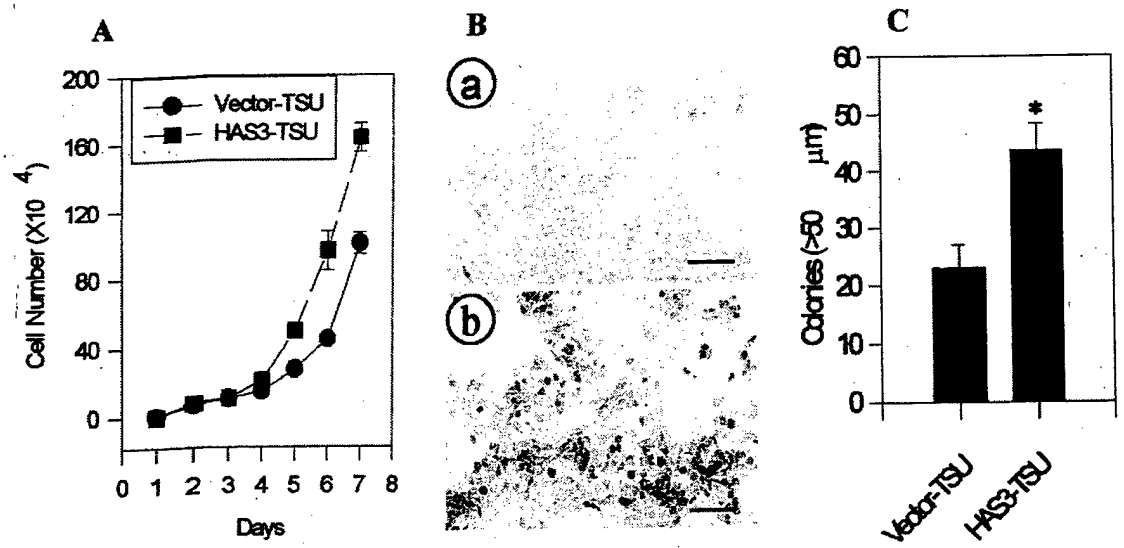

Fig. 4. *In vitro* growth pattern of vector-TSU and HAS3-TSU cells. *A*, cell growth curves for the transfected TSU cells are shown. The cells were plated in 24-well dishes, and the cell number was determined at the indicated times. Although the rate of cell growth was the same at low densities, at higher densities, the HAS3-TSU cells grew faster than the vector-TSU cells. Three independent experiments yielded similar results. *B*, transfected cells at high density were stained for hyaluronan. The transfected cells were grown to confluence, briefly fixed in formaldehyde, and stained for hyaluronan with b-HABP, followed by peroxidase-labeled streptavidin and finally a substrate for peroxidase that gives a red color. The vector-TSU cells (*part a*) formed a confluent monolayer with little hyaluronan staining, whereas the HAS3-TSU cells (*part b*) formed numerous multilayered clusters that stain for hyaluronan (*bar*, 100 μm). *C*, anchorage-independent growth of the transfected cells is shown. Equal numbers of vector-TSU and HAS3-TSU cells were cultured in soft agar for 2 weeks, and the number of colonies were counted with Omnicon Image Analysis system. The HAS3-TSU cells formed a greater number of colonies larger than 50 μm than did the vector-TSU cells (*, $P < 0.05$). This experiment was performed in triplicate.

nucleopore filters by more than 300% as compared with conditioned medium from control cells (Fig. 5*B*). These results further suggest that the hyaluronan produced by HAS3-TSU cells could exert a stimulatory effect on endothelial cells.

The Growth of Transfected Cells on the Chicken Chorioallantoic Membrane. To determine whether the increased growth rate of HAS3-TSU cells *in vitro* also occurred *in vivo*, we examined their growth on the chorioallantoic membranes of chicken eggs. In this experiment, equal numbers of vector-TSU and HAS3-TSU cells were placed on the chorioallantoic membranes of 10-day-old chicken embryos and allowed to grow for 5 days. The xenografts showed a striking divergence in morphology. The vector-TSU cells formed rounded, nodular xenografts that grew out of the membrane surface, with necrotic tissue in the center, whereas the HAS3-TSU cells gave rise to xenografts with a dispersed morphology within the membrane and without any obvious signs of necrosis. As shown in Fig. 6, *A* and *B*, the HAS3-TSU xenografts were significantly larger than those of the vector-TSU cells. Histological examination of the xenografts revealed that, whereas the vector-TSU cells were compact, the HAS3-TSU cells were more dispersed with increased intercellular spaces (data not shown). These results suggested that overexpression of hyaluronan enhanced the tumor growth on the chorioallantoic membrane system.

HAS3 Promotes the Primary Growth of TSU Cells but Not Metastasis in Nude Mice. The *in vivo* growth characteristics of these cells were further examined by injecting them s.c. into nude mice. After 2 weeks, the xenografts formed by HAS3-TSU cells grew at a faster rate and appeared to be more vascularized than the control cells. After 3 weeks of growth, the HAS-3 xenografts were three times larger than those formed by the vector-TSU cells (Fig. 7, *A* and *B*), suggesting that HAS3 promotes the growth of TSU tumor cells in mice. These results are consistent with those obtained from the chicken chorioallantoic membrane system.

However, when transfected cells were injected into the tail veins of nude mice (five mice/group), no lung metastases were detected with either cell type. Thus, the overexpression of hyaluronan by itself is not sufficient to induce metastatic behavior in TSU cells.

Increased Extracellular Hyaluronan and Angiogenesis in HAS3-TSU Xenografts. The xenografts from nude mice were processed for histology, and the resulting sections were stained for hyaluronan (Fig. 8*A*). Although the xenografts varied from region to region, in general, the cells in the vector-TSU xenografts were relatively homogeneous and compact, and most of the hyaluronan appeared to be present in the cytoplasm of the cells (Fig. 8*A*). In contrast, the HAS3-TSU cells formed small clusters or nests of cells that were

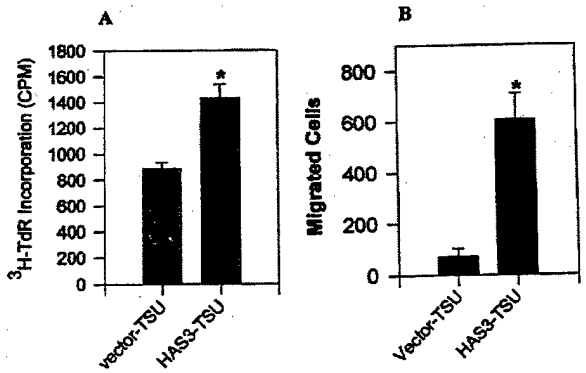

Fig. 5. Effect of conditioned media from vector-TSU and HAS3-TSU cells on endothelial cells. *A*, effects of conditioned media on the proliferation of endothelial cell are demonstrated. ABAE cells were cultured for 36 h in the presence of conditioned media from either vector-TSU or HAS3-TSU cells, pulsed with [^{3}H]thymidine for 8 h, harvested, and processed for incorporated radioactivity. The conditioned media from HAS3-TSU cells stimulated the ABAE cells to a greater extent than that from vector-TSU cells. *B*, effects of conditioned medium on the migration of endothelial cells is shown. Aliquots containing 5×10^3 ABAE cells were added to bottom wells of a 48-well Boyden chamber, covered with a nucleopore membrane, and then treated with 50 μl of conditioned medium for 2 h. The membrane was stained with Hema 3 and placed on a slide, and the migrated cells were counted in 10 random fields. Conditioned medium from HAS3-TSU cells significantly increased the migration of the endothelial cells as compared with that from the vector-TSU cells ($P < 0.05$).

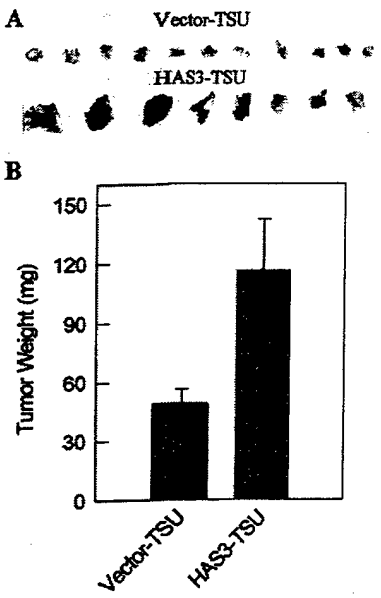

Fig. 6. Growth of transfected TSU cells on the chicken chorioallantoic membrane. Samples of vector-TSU and HAS3-TSU cells (2×10^6 cells) were placed on the chorioallantoic membranes of 10-day-old chicken embryos (15 eggs/group), incubated at 37°C for 5 days, and then photographed. *A*, the xenografts of vector-TSU cells (*top row*) and HAS3-TSU cells (*bottom row*) from the chorioallantoic membrane are shown. The vector-TSU xenografts formed compact nodules, whereas the HAS3-TSU xenografts were more spread out and larger. *B*, the weights of the HAS3-TSU xenografts were significantly greater than that of the vector-TSU cells ($P < 0.05$).

surrounded by a matrix rich in hyaluronan (Fig. 8*A*). Such structures were not observed in the control-TSU xenografts.

The extent of angiogenesis in these xenografts was examined by staining for mouse endothelial cells using antibodies to CD31. Fig. 8*B* shows that there was strong positive staining in HAS3-TSU xenografts as compared with the control vector-TSU xenografts. The number of vessels in 10–15 random fields was significantly higher in the HAS3-TSU xenografts than in the control xenografts (Fig. 8*C*). This suggests that increased levels of hyaluronan can stimulate angiogenesis in mice, and this may, in part, account for the faster growth rate of tumors formed by HAS3-TSU cells.

DISCUSSION

In this study, we have characterized human HAS3 with regard to both its structure and its function in tumor progression. On the basis of its deduced amino acid sequence, HAS3 shares significant homology with HAS1 and HAS2, containing a signal peptide as well as six transmembrane regions strongly suggesting that it is associated with the plasma membrane. Its enzymatic activity was demonstrated by the fact that TSU cells transfected with expression vectors for HAS3 produced larger amounts of hyaluronan as determined by histochemical staining, dot blot analysis, and quantitative ELISA. These findings are consistent with earlier studies of HAS proteins (12–19).

This study also suggested that stimulation of hyaluronan synthesis in TSU cells by transfecting them with HAS3 expression vectors enhanced their growth both in chicken embryos and in nude mice. This enhanced tumor growth appeared to be attributable to two distinct mechanisms. The first involved a direct effect on the tumor cells themselves, as indicated by the fact that in tissue culture, HAS3-transfected cells grew at a faster rate at high density. The second mechanism promoting tumor growth rate resulted from an increase in vascularization, as reflected by the greater density of blood vessels in xenografts from nude mice. Together, these two factors contribute to the increased tumor growth rate.

At present, we believe that the effects of HAS3 transfection on TSU cell phenotype are a direct consequence of increased hyaluronan synthesis. Along these lines, it is important to note that HAS3 overexpression increases the production of both secreted and cell-associated hyaluronan. These two pools of hyaluronan may have different effects on cell behavior. This was suggested by preliminary experiments in which we found that the addition of high molecular weight hyaluronan to cultures of vector-TSU or HAS3-TSU cells had no obvious effect on their growth rates (data not shown). We believe that under these specific conditions, free hyaluronan of high molecular weight did not affect the behavior of these cells. Rather, we believe that it was the cell-associated fraction of hyaluronan induced by HAS3 that played a more important role in stimulating cell growth. However, we cannot eliminate the possibility that hyaluronan of the appropriate size and concentration may indeed influence the behavior of TSU cells, similar to the effects that it has on endothelial cells (27, 28). It is also possible that HAS3 may have effects on the TSU cells independent of its function to promote hyaluronan synthesis; *e.g.*, HAS3 could influence the interaction of the plasma membrane with elements of the cytoskeleton and thereby alter cell behavior.

The hyaluronan on the surface of cultured cells can form a pericellular coat that can be directly visualized by its ability to exclude small particles such as erythrocytes (30). In the case of rat fibrosarcoma cells, this coat is composed of small, microvilli-like projections that extend out from the surface of the cells to which the hyaluronan is attached (31). This pericellular coat could stimulate the growth of cells by several different mechanisms. One possible mechanism is that it disrupts intercellular junctions and thereby allows the cells to detach from the substrate so that they can divide and occupy new space (32–34). This would allow cells to overcome contact inhibition of growth that is characteristic of TSU cells and allow them to from multilayers at high-density cultures as we have observed. Another possibility is that the hyaluronan interacts with receptors on the surfaces of cells such as CD44 or RHAMM to influence their migratory and proliferative behavior (35, 36).

Extracellular hyaluronan can also stimulate cell proliferation by

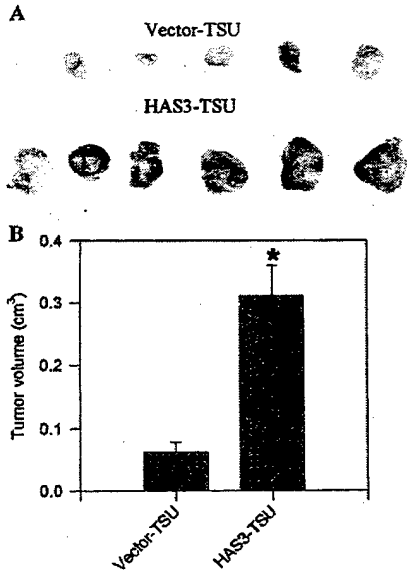

Fig. 7. Xenografts formed by transfected TSU cells in nude mice. *A*, the appearance of xenografts formed in nude mice is shown. Mice received injections of 2×10^6 vector-TSU cells (*top*) or HAS3-TSU cells (*bottom*), and the xenografts were harvested 21 days later. The HAS3-TSU xenografts were larger than those of the vector-TSU cells. *B*, the weights of the HAS3-TSU xenografts were significantly greater than that of the vector-TSU ($P < 0.05$).

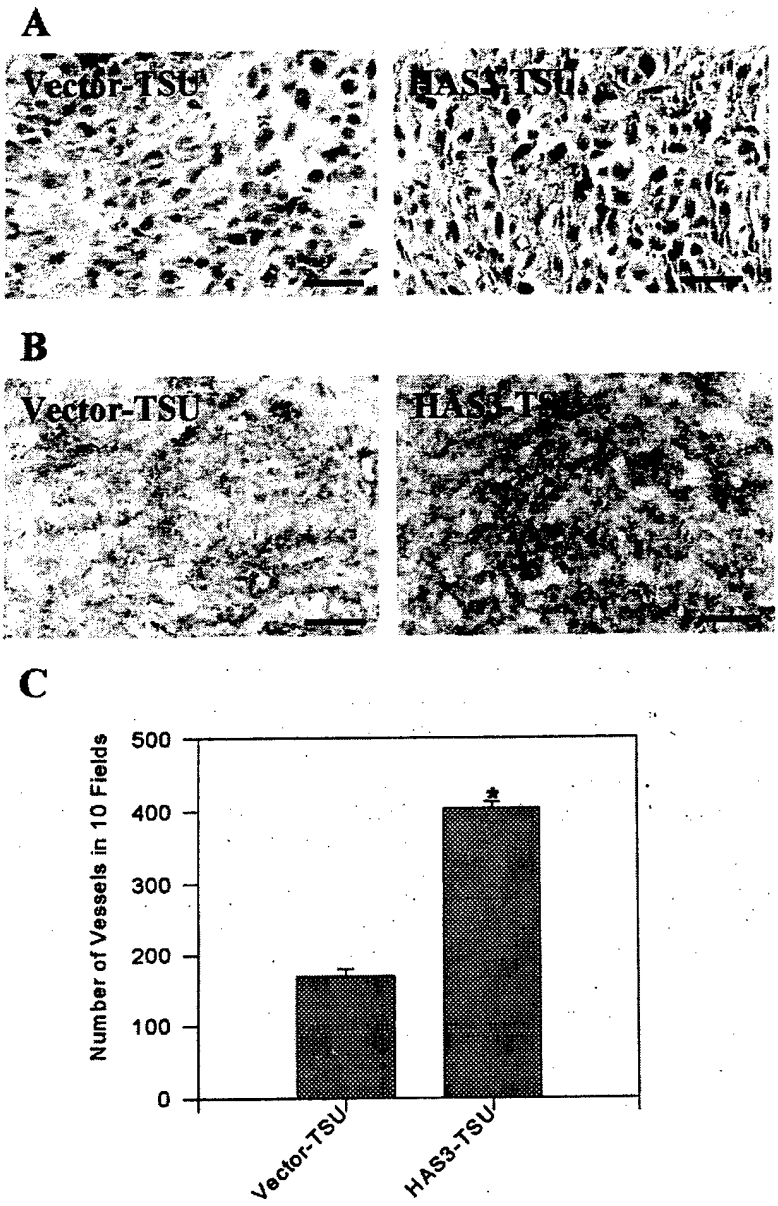

Fig. 8. Staining of xenografts for hyaluronan and endothelial cells. *A*, paraffin sections of vector-TSU and HAS3-TSU xenografts from nude mice were stained for hyaluronan (*red*) and counter-stained with hematoxylin (*blue*). A representative section of a vector-TSU xenograft shows that most of the hyaluronan staining was associated with the cytoplasm of the cells, whereas in a similar section from a HAS3-TSU xenograft, the cells were present in small clusters, surrounded by a stroma rich in hyaluronan. Although the microscopic morphology of the xenografts varied from region to region, the hyaluronan-rich stroma was prevalent in the HAS3-TSU xenografts and absent from the vector-TSU xenografts. *Bar*, 50 μm. *B*, cryostat sections of the xenografts were stained for endothelial cells using an antibody against mouse CD31. Representative fields show that xenografts formed from HAS3-TSU cells have a higher concentration of endothelial cells than those from vector-TSU cells. *Bar*, 100 μm. *C*, the number of blood vessels in 10 random fields from three samples of each group are shown. The HAS3-TSU xenografts had a significantly higher concentration of blood vessels than that of the vector-TSU cells ($P < 0.05$).

increasing the flow of nutrients. Indeed, the extracellular hyaluronan apparent in xenografts of HAS3-TSU cells in nude mice could serve as conduits through which nutrients diffuse to support cells located some distance from the blood supply and thus facilitate their growth. In the xenografts of vector-TSU cells that lacked these hyaluronan rich spaces, the tumor cells formed a continuous mass and were more susceptible to necrosis. Along these lines, extracellular hyaluronan is prominent in the lower regions of most, if not all, stratified epithelium, where it is believed to maintain spaces so that nutrients can diffuse to the more superficial epithelial cells (37, 38).

Hyaluronan also appeared to promote vascularization that is clearly important in regulating tumor growth (39, 40). This was indicated by our observation that xenografts of HAS3-TSU cells formed in nude mice had a greater density of blood vessels than did control xenografts. Part of this increased vascularization may be attributable to the pericellular spaces generated by the hyaluronan that provides space that facilitates the invasion of endothelial cells. In addition, the hyaluronan itself can stimulate the migration of endothelial cells. This was also indirectly suggested by experiments showing that conditioned media from the HAS3-transfected cells stimulated the growth and migration of cultured endothelial cells. This is consistent with the earlier studies of West *et al.* (27, 28) who have shown that oligosaccharide fragments of hyaluronan stimulated the formation of new blood vessels in the chorioallantoic membrane of chicken embryos.

Although the results of this study suggest that overexpression of HAS3 in TSU prostate cancer cells promotes their tumorigenicity, there are some aspects that appear to contradict the findings of other studies; *e.g.*, although we found that TSU transfectants grew faster in culture, Kosaki *et al.* (20) found no such increase in the growth of HT1080 cells transfected with HAS2 under anchorage-dependent conditions; however, these cells did form larger colonies in suspension culture. We believe that this difference may be attributable in part to the different target cells that were used in these studies. The TSU cells used as targets in this study are of epithelial origin, whereas HT1080 cells are derived from a fibrosarcoma of connective tissue cells. This could also account for the differences seen with regard to growth behavior and the production of hyaluronan in the connective tissue and their ability to stimulate angiogenesis. Alternatively, the

differences could be attributed to the characteristics of the particular HASs that were used in these studies, because they differ with respect to both their synthetic activity as well as the size of the hyaluronan that they produce (16–18).

Another apparent discrepancy was our observation that transfection of TSU cells with HAS3 did not appear to stimulate their ability to form lung metastases in nude mice. In contrast, we had reported previously (3) that the levels of hyaluronan on the surface of B16 cells were directly correlated with their metastatic behavior. Similarly, Itano *et al.* (21) found that transfection of FM3A with HAS1 enhanced their metastatic properties. Again, we believe that these divergent results were attributable to the different cell types that were used as targets for transfection. In the case of B16 and FM3A, these cell lines originally possessed the ability to undergo metastasis, and stimulation of hyaluronan synthesis in these cells enhanced this innate property. In contrast, TSU cells appeared to lack this ability (at least in nude mice), and increased hyaluronan synthesis, by itself, is not sufficient to promote metastatic properties. Clearly, the process of metastasis is a complex phenomenon involving the collaboration of many molecules. Although the production of hyaluronan is one of the factors, it is not sufficient for tumor metastasis in the case of TSU cells.

In conclusion, the results of this study indicate that HAS3 expression plays a role in tumor progression and are consistent with earlier studies demonstrating a correlation between hyaluronan levels and tumorigenicity. Furthermore, the hyaluronan may be acting through several different mechanisms, including: (*a*) a direct effect on the growth of the tumor cells themselves; (*b*) the formation of extracellular conduits through which nutrients can flow; and (*c*) the stimulation of blood vessel growth. However, these effects depend upon the particular cell type and the specific environment. Given the complexity of the effects of hyaluronan, it may be difficult to predict exactly how it will influence the behavior of tumor cells. In the case of TSU cells, hyaluronan may be more of a facilitator of tumor growth rather than an instigator of metastasis.

REFERENCES

1. Toole, B. P., Biswas, C., and Gross, J. Hyaluronate and invasiveness of the rabbit V2 carcinoma. Proc. Natl. Acad. Sci. USA, *76:* 6299–6303, 1979.
2. Kimata, K., Honma, Y., Okayama, M., Oguri, K., Hozumi, M., and Suzuki, S. Increased synthesis of hyaluronic acid by mouse mammary carcinoma cell variants with high metastatic potential. Cancer Res., *43:* 1347–1354, 1983.
3. Zhang, L., Underhill, C. B., and Chen, L. Hyaluronan on the surface of tumor cells is correlated with metastatic behavior. Cancer Res., *55:* 428–433, 1995.
4. Marotta, M., D'Armiento, F. P., Martino, G., Donato, G., Nazzaro, A., Vecchione, R., and Rosati, P. Glycosaminoglycans in human breast cancer: morphological and biochemical study. Appl. Pathol., *3:* 164–169, 1985.
5. Coppes, M. J. Serum biological markers and paraneoplastic syndromes in Wilm's tumor. Med. Pediatr. Oncol., *21:* 213–221, 1993.
6. Horai, T., Nakamura, N., Tateshi, R., and Hattori, S. Glycosaminoglycans in human lung cancer. Cancer (Phila.), *48:* 2016–2021, 1981.
7. Roboz, J., Greaves, J., Silides, D., Chahinian, A. P., and Holland, J. F. Hyaluronic acid content of effusions as a diagnostic aid for malignant mesothelioma. Cancer Res., *45:* 1850–1854, 1985.
8. Kojima, J., Nakamura, N., Kanatani, M., and Omori, K. The glycosaminoglycans in human hepatic cancer. Cancer Res., *35:* 542–547, 1975.
9. Azumi, N., Underhill, C. B., Kagan, E., and Sheibani, K. A novel biotinylated probe specific for hyaluronate: its diagnostic value in diffuse malignant mesothelioma. Am. J. Surg. Pathol., *16:* 116–121, 1992.
10. Dahl, I. M. S., and Laurent, T. C. Concentration of hyaluronan in serum of untreated cancer patients reference to patients with mesothelioma. Cancer (Phila.), *62:* 326–330, 1988.
11. Frebourg, T., Lerebours, G., Delpech, B., Benhamou, D., Bertrand, P., Maingonnat, C., Boutin, C., and Nouvet, G. Serum hyaluronate in malignant pleural mesothelioma. Cancer (Phila.), *59:* 2104–2107, 1987.
12. Shyjan, A. M., Heldin, P., Butcher, E. C., Yoshino, T., and Briskin, M. J. Functional cloning of the cDNA for a human hyaluronan synthase. J. Biol. Chem., *271:* 23395–23399, 1996.
13. Watanabe, K., and Yamaguchi, Y. Molecular identification of a putative human hyaluronan synthase. J. Biol. Chem., *271:* 22945–22948, 1996.
14. Itano, N., and Kimata, K. Molecular cloning of human hyaluronan synthase. Biochem. Biophys. Res. Commun., *222:* 816–820, 1996.
15. Itano, N., and Kimata, K. Expression cloning and molecular characterization of HAS protein, a eukaryotic hyaluronan synthase. J. Biol. Chem., *271:* 9875–9878, 1996.
16. Spicer, A. P., Olson, J. S., and McDonald, J. A. Molecular cloning and characterization of a cDNA encoding the third putative mammalian hyaluronan synthase. J. Biol. Chem., *272:* 8957–9861, 1997.
17. Spicer, A. P., and McDonald, J. A. Characterization and molecular evolution of a vertebrate hyaluronan synthase gene family. J. Biol. Chem., *273:* 1923–1932, 1998.
18. Spicer, A. P., and Nguyen, T. K. Mammalian hyaluronan synthases: investigation of functional relationships *in vivo*. Biochem. Soc. Trans., *27:* 109–115, 1999.
19. Itano, N., Sawai, T., Yoshida, M., Lenas, P., Yamada, Y., Imagawa, M., Shinomura, T., Hamaguchi, M., Yoshida, Y., Ohnuki, Y., Miyauchi, S., Spicer, A. P., McDonald, J. A., and Kimata, K. Three isoforms of mammalian hyaluronan synthases have distinct enzymatic properties. J. Biol. Chem., *274:* 25085–25092, 1999.
20. Kosaki, R., Watanabe, K., and Yamaguchi, Y. Overproduction of hyaluronan by expression of the hyaluronan synthase Has2 enhances anchorage-independent growth and tumorigenicity. Cancer Res., *59:* 1141–1145, 1999.
21. Itano, N., Sawai, T., Miyaishi, O., and Kimata, K. Relationship between hyaluronan production and metastatic potential of mouse mammary carcinoma cells. Cancer Res., *59:* 2499–2504, 1999.
22. Chen, C., and Okayama, H. High-efficiency transformation of mammalian cells by plasmid DNA. Mol. Cell. Biol., *7:* 2745–2752, 1987.
23. Underhill, C. B., and Zhang, L. Analysis of hyaluronan using biotinylated hyaluronan-binding proteins. Methods Mol. Biol., *137:* 441–447, 1999.
24. Culty, M., Shizari, M., Nguyen, H. A., Clarke, R., Thompson, E. W., and Underhill, C. B. Degradation of hyaluronan and expression of CD44 by human breast cancer cell lines correlate with their invasive potential. J. Cell. Physiol., *160:* 275–286, 1994.
25. Falk, W., Goodwin, R. H., and Leonard, E. J. A 48-well micro chemotaxis assembly for rapid and accurate measurement of leukocyte migration. J. Immunol. Methods, *33:* 239–247, 1980.
26. Yang, B., Yang, B. L., Savani, R. C., and Turley, E. A. Identification of a common hyaluronan binding motif in the hyaluronan binding proteins RHAMM, CD44 and link protein. EMBO J., *13:* 286–296, 1994.
27. West, D. C., Hampson, I. N., Arnold, F., and Kumar, S. Angiogenesis induced by degradation products of hyaluronic acid. Science (Wash. DC), *228:* 1324–1326, 1985.
28. West, D. C., and Kumar, S. The effect of hyaluronate and its oligosaccharides on endothelial cell proliferation and monolayer integrity. Exp. Cell Res., *183:* 179–196, 1989.
29. Feinberg, R. N., and D. C. Beebe. Hyaluronate in vasculogenesis. Science (Wash. DC), *220:* 1177–1179, 1983.
30. Underhill, C. B., and Toole, B. P. Transformation-dependent loss of the hyaluronate-containing coats of cultured cells. J. Cell. Physiol., *110:* 123–128, 1982.
31. Koshiishi, I., Shizari, M., and Underhill, C. B. CD44 mediates the adhesion of platelets to hyaluronan. Blood, *84:* 390–396, 1994.
32. Brecht, M., Mayer, U., Schlosser, E., and Prehm, P. Increased hyaluronate synthesis is required for fibroblast detachment and mitosis. Biochem. J., *239:* 445–450, 1986.
33. Lark, M. W., and Culp, L. A. Selective solubilization of hyaluronic acid from fibroblast substratum adhesive sites. J. Biol. Chem., *257:* 14073–14080, 1982.
34. Abatangelo, G., Cortivo, R., Martelli, M., and Vecchia, P. Cell detachment mediated by hyaluronic acid. Exp. Cell Res., *137:* 73–78, 1982.
35. Zhang, S., Chang, M. C., Zylka, D., Turley, S., Harrison, R., and Turley, E. A. The hyaluronan receptor RHAMM regulates extracellular-regulated kinase. J. Biol. Chem., *273:* 11342–11348, 1998.
36. Bourguignon, L. Y., Shu, H., Shao, L., and Chen, Y. W. CD44 interaction with Tiam1 promotes Rac1 signaling and hyaluronic acid-mediated breast tumor migration. J. Biol. Chem., *275:* 1829–1338, 2000.
37. Alho, A. M., and Underhill, C. B. The hyaluronate receptor is preferentially expressed on proliferating epithelial cells. J. Cell Biol., *108:* 1557–1565, 1989.
38. Underhill, C. B. The interaction of hyaluronate with the cell surface: the hyaluronate receptor and the core protein. Ciba Found. Symp., *143:* 87–106, 1989.
39. Folkman, J. New perspectives in clinical oncology from angiogenesis research. Eur. J. Cancer, *32:* 2534–2539, 1996.
40. Folkman, J., and D'Amore, P. A. Blood vessel formation: what is its molecular basis? Cell, *87:* 1153–1155, 1996.

#4233 Triptolide, a potent antitumor agent. Shanmin Yang, Jinguo Chen, Xue-Ming Xu, Luping Wang, Shimin Zhang, Xu-Fang Pei, Jing Yang, Charles B. Underhill, and Lurong Zhang. *the Cell and Tumor Key Lab of China Education Ministry at Xiamen University, Xiamen, China, Georgetown University Medical Center, Washington, DC, and PowerTech Inc., Bethesda, MD.*

Triptolide (TPL) is a compound (MW 360) purified from the herb Tripterygium wilfordii Hook F that has been used in China as a natural medicine for hundreds of years. In China, clinical trials have indicated that TPL could achieve complete or partial remission in patients with leukemia. In the present study, we examined the effects of TPL on cell lines derived from human cancers of the breast, prostate, stomach and liver. In addition, mouse B16 melanoma cells were used as an experimental model of metastasis. In the case of cultured tumor cells, TPL at 4 ng/ml inhibited cell growth to a similar extent as taxol at 100 ng/ml both under anchorage-dependent and -independent conditions. When mice with tumor xenografts formed by several different cell lines were injected i.v. with TPL at a dose of 0.25 mg/kg/ twice a week, the sizes of the tumor xenografts were reduced to 10-50% of the controls. This was comparable or superior to that achieved with the commonly used chemotherapeutic drugs adrimycin, cisplatin and mitomycin. Importantly, TPL could inhibit both spontaneous and experimental metastasis. Additional studies revealed that treatment of tumor cells with 10 ng/ml of TPL for 24 hours resulted in decreased levels of c-myc, cyclin A/cdk2 and cyclin B/cdc2 while increasing the level of cleaved PARP, an indicator of apoptosis. Furthermore, TPL also decreased the telomerase activity as measured by both the TRAP assay and PicoGreen staining. These results strongly suggest that TPL can potentially be developed as a new anti-tumor/metastasis agent.

Proceedings of the American Association for Cancer Research • Volume 43 • March 2002

#3962 Overexpression of tumor necrosis factor-stimulated gene-6 protein (TSG-6) suppresses tumor growth *in vivo*. Jinguo Chen, Xue-Ming Xu, Shanmin Yang, Luping Wang, Charles B. Underhill, and Lurong Zhang. *Georgetown University Medical Center, Washington, DC, The Cell and Tumor Key Lab of China Education Ministry at Xiamen University; Xiamen, China, and Beijing General Hospital, Beijing, China.*

Tumor necrosis factor-stimulated gene-6 protein (TSG-6) is an anti-inflammatory factor that is produced in response to TNF and contains a link module that allows it to bind hyaluronan. In this study, we examined the effects of overexpression of TSG-6 on tumor progression. The cDNA coding for human TSG-6 gene (782bp) was cloned, inserted into an expression vector (pSecTag2/Hygro B) and transfected into TSU human prostate cancer cells. The positive clones were identified by RT-PCR and the biological activity of the TSG-6 protein was confirmed by its ability to bind hyaluronan. The TSG-6 positive clones were then pooled and compared with control cells (transfected with vector) with regard to cell behaviors. In culture, the TSG-6 transfected TSU cells grew at the same rate as control cells as measured by cell number and by incorporation of radioactive thymidine. However, when the cells were inoculated on the chorioallantoic membrane of chicken embryos, the TSG-6 transfected TSU cells grew at a slower rate than the control cells (mean xenograft weight in TSG-6 16.3 mg vs. control 39.6 mg). Similarly, when cells were injected s.c. into nude mice, the xenografts formed by the TSG-6-transfected cells were smaller than that of the control cells (mean xenograft weight 0.72 g vs. 2.16 g). Western Blot analysis of lysates from these xenografts indicated that the TSG-6 transfected cells had increased levels of Fas, cleaved caspase 8 and cleaved PARP, but no change in the levels of cyclin D1, B1, Rb, ERK. These preliminary results suggest that TSG-6 could function as a tumor suppressor *in vivo*, in part, through the induction of apoptosis.

#4404 Targeted hyaluronan binding peptide inhibits the growth of ST88-14 Schwann cells. Yixin Chen, Shuigen Hong, Xiaolin Chen, Shanmin Yang, Ningfei Liu, Xu-Fang Pei, Luping Wang, Xue-Ming Xu, Jinguo Chen, Charles B. Underhill, and Lurong Zhang. *The Cell and Tumor Key Lab of China Education Ministry at Xiamen University, Xiamen, China, and Georgetown University Medical Center, Washington, DC.*

We have reported that the hyaluronan (HA) binding proteins/peptides possess anti-tumor effect, in part, due to the induction of apoptosis and p53. The loss of neurofibromin, a tumor suppressor corded by NF1 (Neurofibromatosis Type 1) gene, results in the accumulation of hyperactive Ras-GTP due to a reduced conversion of active Ras-GTP to inactive Ras-GDP, which turns on uncontrolled mitogenic signals in the nucleus. Therefore, neurofibromatosis can be regarded as a disease resulting from the disruption of the balance between cell proliferation and apoptosis. To determine if the abnormality of neurofibromatosis can be interrupted by HA binding peptide, a naturally existing HA binding peptide, tachyplesin with RGD domain (for a better targeting) and its scramble peptide were synthesized. When ST88-14 Schwann cells were treated with this targeted peptide for 24 hours, the cells underwent apoptosis and began to die. The 3H-TdR incorporation rate of targeted HA binding peptide treated cells was greatly reduced compared to that of the control peptide treated cells. This inhibitory effect was in a dose-dependent manner. Similarly, the ability to form colony in soft agar was also remarkably reduced. Western blot analysis showed that the cell cycle key molecules, such as cyclin B1 and cdc2, were reduced. In addition, the targeted HA binding peptide could reduce the phosphorylation of mitogen-activated protein kinase. The data suggest that the targeted HA binding peptide could inhibit the growth of ST88-14 Schwann cells via suppression of some key molecules in cell proliferation process.

Proceedings of the American Association for Cancer Research • Volume 43 • March 2002

#5364 Peptides derived endostatin and angiostatin inhibits tumor growth. Xueming Xu, Jinguo Chen, Luping Wang, Xue-Fang Pei, Shanmin Yang, Charles B. Underhill, and Lurong Zhang. *Georgetown University, Washington, DC.*

Endostatin and angiostatin are well-known anti-tumor/angiogenesis agents. We have found that there are several hyaluronan (HA) binding motifs existing in these two proteins. In previous studies, we have found that HA binding proteins / peptides inhibited the growth of tumor cells. In this study, two peptides with HA binding motifs derived from endostatin and angiostatin were tested to confirm that the HA binding motifs are the critical effector in the bioactivity of their parental molecules. Two peptides that containing 2-3 HA binding motifs and NGR homing domain or the control scramble peptide were chemically synthesized. When the peptides were added to endothelial cells (HUVEC and ABAE) or tumor cells (TSU prostate or MDA435 breast cancer), they inhibited the cell growth in a dose-dependent manner. When 100 μg of peptides was tropically administrated to TSU tumors grown on chorioallantoic membrane of chicken embryo, the sizes of tumors in the peptide-treated groups were smaller than the control, while the development of chick embryos were not affected. The results of Western blot and flow cytometry analysis indicated that the peptides could trigger the depolarization of mitochondrial, induce the expression of p16 and p21 and increase the cleaved caspase 8. It seems that the HA binding motifs in endostatin and angiostatin are the key factor for the anti-tumor/angiogenesis effects of their parental proteins.